



U.S. DEPARTMENT OF
ENERGY



**Photo Credit: I. Tsukerman, Seefeld,
Austria, January, 2009**



Latest Progress in Nanoplasmonics and Spaser

Mark I. Stockman

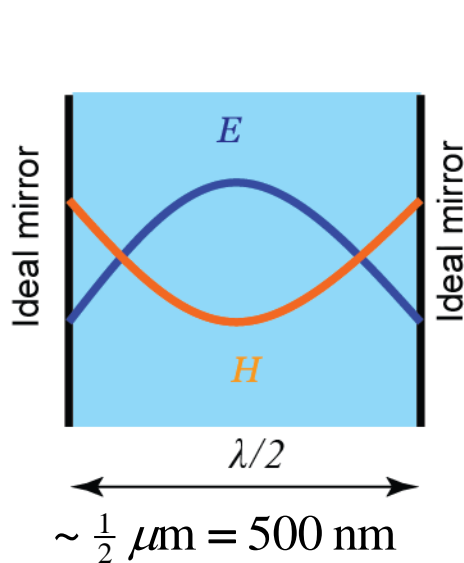
**Center for Nano-Optics (CeNO) and Department of Physics and Astronomy,
Georgia State University, Atlanta, GA, USA**

• **Introduction: Plasmonics and Nano-confinement of Optical Energy**

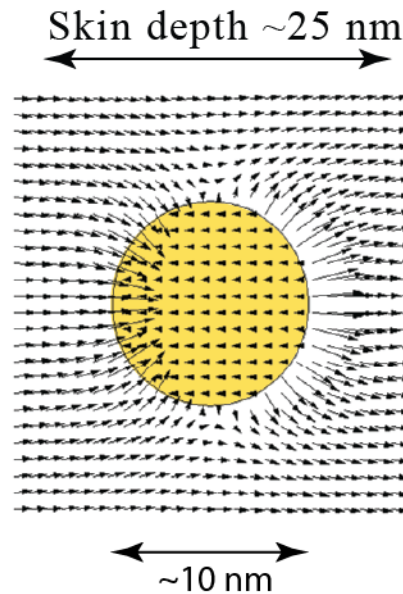
- Nanoplasmonic Resonances and their Frequencies (Colors)
- Localized Surface Plasmons and Plasmonic Hot Spots
- Plasmonic Enhancement and Ultrafast Nature of Plasmonics
- Nanolenses
- Applications of Nanoplasmonics
- Sensing and Detection
- Plasmonic Nanoscopy
- Spaser as an Ultrafast Quantum Generator and Nanoamplifier: Introduction
- Spaser as an Ultrafast Quantum Generator and Nanoamplifier: Theory
- Spaser as an Ultrafast Quantum Generator and Nanoamplifier: Experiment

Nanoplasmonics in a nano-nutshell

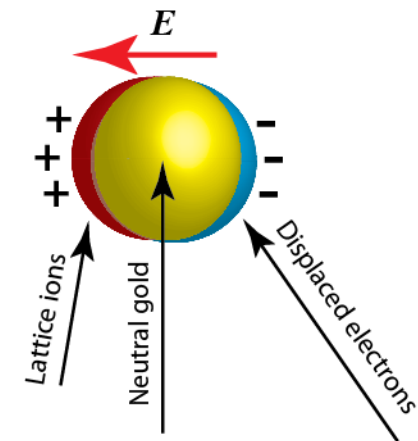
Concentration of optical energy on the nanoscale



Photon: Quantum of electromagnetic field

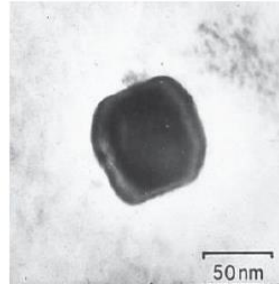


Surface Plasmon: Quantum of electromechanical oscillator



- Introduction: Plasmonics and Nano-confinement of Optical Energy
- **Nanoplasmonic Resonances and their Frequencies (Colors)**
- Localized Surface Plasmons and Plasmonic Hot Spots
- Plasmonic Enhancement and Ultrafast Nature of Plasmonics
- Adiabatic Nanofocusing
- Nanolenses
- Applications of Nanoplasmonics
- Sensing and Detection
- Plasmonic Nanoscopy
- Spaser as an Ultrafast Quantum Generator and Nanoamplifier: Introduction
- Spaser as an Ultrafast Quantum Generator and Nanoamplifier: Theory
- Spaser as an Ultrafast Quantum Generator and Nanoamplifier: Experiment

Lycurgus Cup (4th Century AD): Roman Nanotechnology

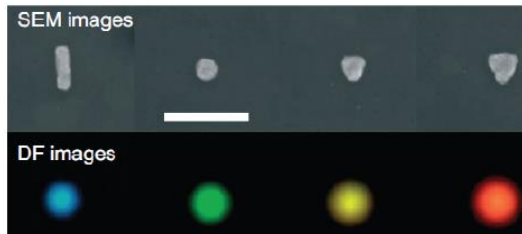
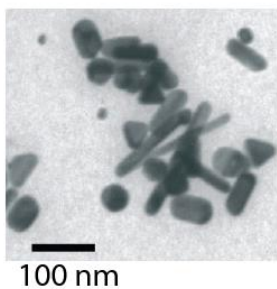
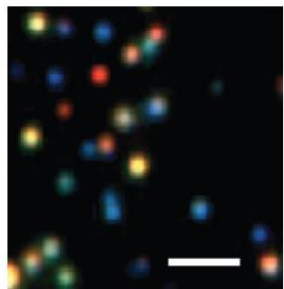


I. Freestone, N. Meeks, M. Sax, and C. Higgitt, *The Lycurgus Cup - a Roman Nanotechnology*, *Gold Bull.* **40**, 270-277 (2007)

Nanoplasmonic colors are very bright. Scattering and absorption of light by them are very strong. This is due to the fact that all of the millions of electrons move in unison in plasmonic oscillations. Nanoplasmonic colors are also eternal: metal nanoparticles are stable in glass: they do not bleach and do not blink. Gold is stable under biological conditions and is not toxic *in vivo*.

© Trustees of British Museum

Colors of Silver Nanocrystals and Gold Nanoshapes



Scanning electron microscopy

Dark field optical microscopy

W. A. Murray and W. L. Barnes, *Plasmonic Materials*, *Adv. Mater.* **19**, 3771-3782 (2007) [Scale bar: 300 nm]

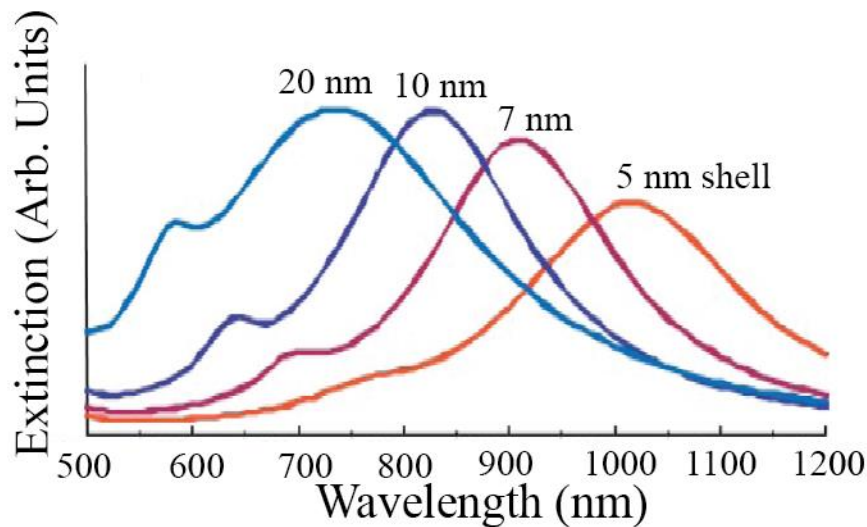
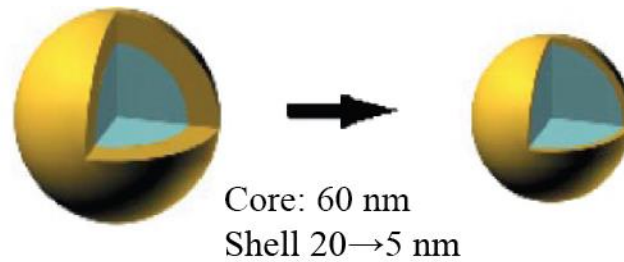
C. Orendorff, T. Sau, and C. Murphy, *Shape-Dependent ...*, *Small* **2**, 636-639 (2006)

Latest Progress in Nanoplasmonics and Spasers

<http://www.phy-astr.gsu.edu/stockman>
E-mail: mstockman@gsu.edu

Siegman School, ICFO p.5
7/28/2016 11:55 AM

When shell becomes progressively thinner comparing to the core, the spectrum of the nanoshell shifts to the red and then to the near-infrared where biological tissues do not absorb



J. L. West and N. J. Halas, *Engineered Nanomaterials for Biophotonics Applications: Improving Sensing, Imaging, and Therapeutics*, *Annu. Rev. Biomed. Eng.* **5**, 285-292 (2003).



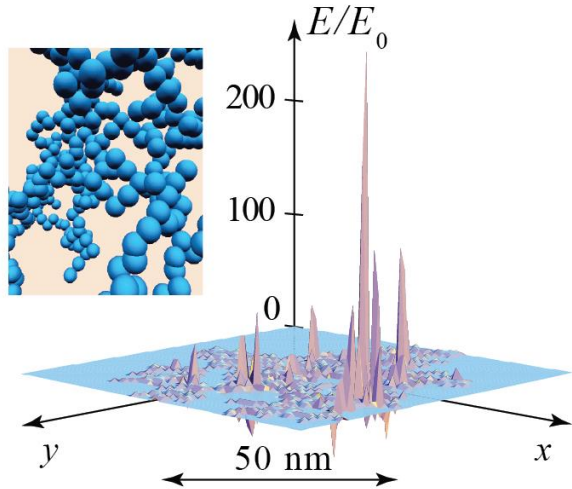
The magnificent nanoplasmonic colors: The windows of La Sainte-Chapelle, Paris

M. I. Stockman, *Nanoplasmonics: The Physics Behind the Applications*, Phys. Today **64**, 39-44 (2011).

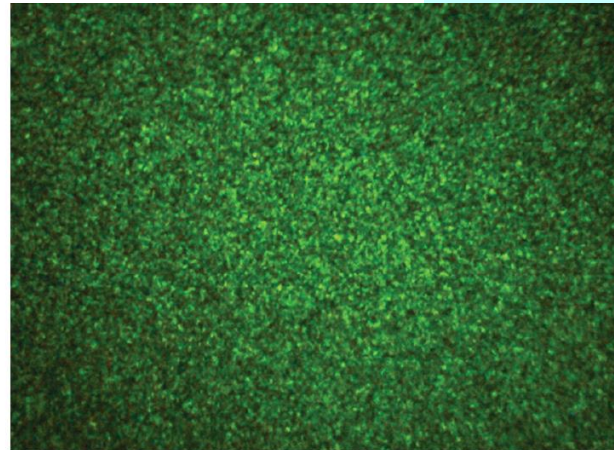
- Introduction: Plasmonics and Nano-confinement of Optical Energy
- Nanoplasmonic Resonances and their Frequencies (Colors)
- **Localized Surface Plasmons and Plasmonic Hot Spots**
- Plasmonic Enhancement and Ultrafast Nature of Plasmonics
- Adiabatic Nanofocusing
- Nanolenses
- Applications of Nanoplasmonics
- Sensing and Detection
- Plasmonic Nanoscopy
- Spaser as an Ultrafast Quantum Generator and Nanoamplifier: Introduction
- Spaser as an Ultrafast Quantum Generator and Nanoamplifier: Theory
- Spaser as an Ultrafast Quantum Generator and Nanoamplifier: Experiment

Plasmonic Near-Field Hot Spots: Happy 22nd Anniversary!

- D. P. Tsai et al., *Phys. Rev. Lett.* **72**, 4149 (1994).
- M. I. Stockman et al., *Phys. Rev. Lett.* **75**, 2450 (1995)
- M. I. Stockman, L. N. Pandey, and T. F. George, *Phys. Rev. B* **53**, 2183 (1996)



M. I. Stockman, L. N. Pandey, and T. F. George, *Phys. Rev. B* 53, 2183 (1996).



50 cm

Random scattering speckles

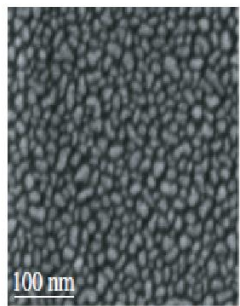
$$R_{\text{Speckle}} \sim \frac{\hat{\lambda}}{A} L$$

R_{Speckle} is speckle size

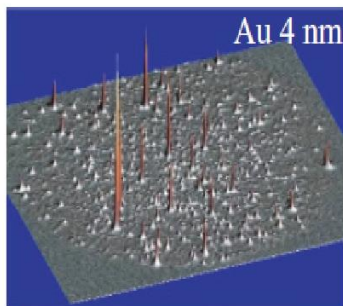
$\hat{\lambda} \sim 100$ nm is reduced wave length

A is laser spot size,

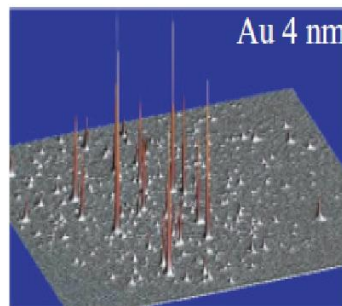
L is distance to the screen



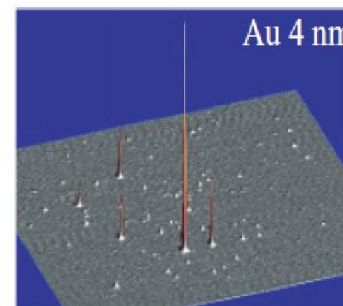
Au 4 nm, $f = 0.53$



$\lambda = 800$ nm, Hot Spots Nb = 617



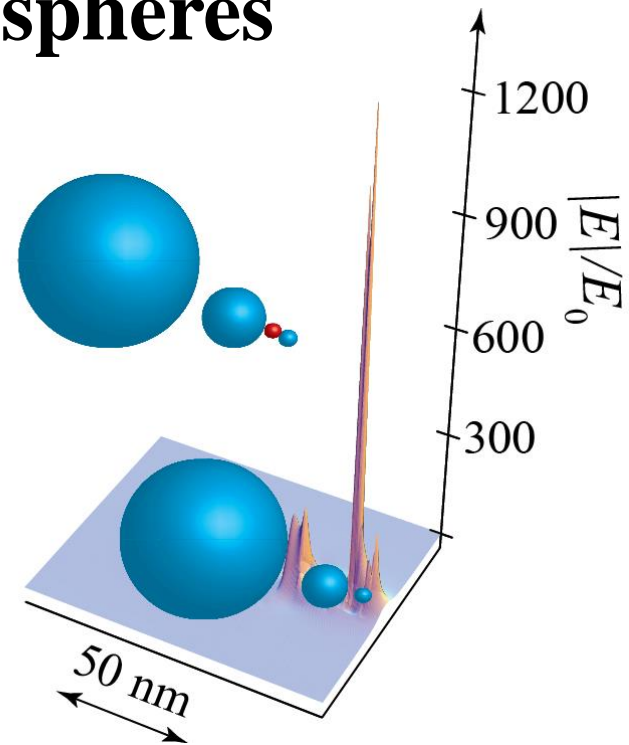
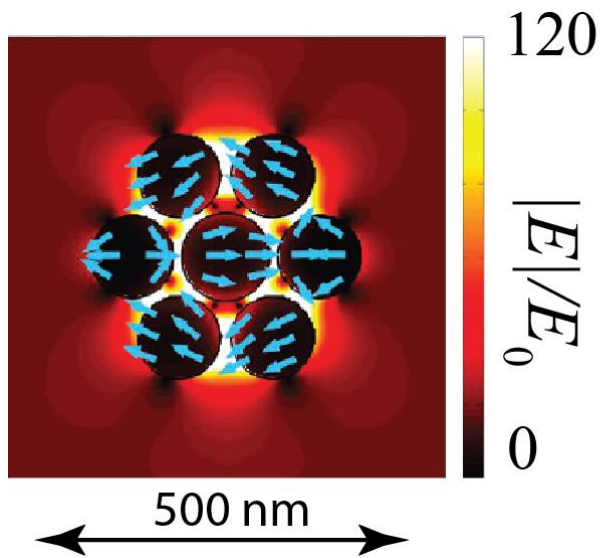
$\lambda = 930$ nm, Hot Spots Nb = 453



$\lambda = 970$ nm, Hot Spots Nb = 402

C. Awada, G. Barbillon, F. Charra, L. Douillard, and J. J. Greffet, *Phys. Rev. B* **85**, 045438 (2012).

Engineered Nanoplasmonic Hot Spots in Small Clusters of Nanospheres



Fano resonance in a nanosphere cluster:

- J. A. Fan et al., *Science* **328**, 1135 (2010)
- M. Hentschel et al., *Nano Lett.* **10**, 2721 (2010)

Self-similar nanosphere nanolens: K. Li, M. I. Stockman, and D. J. Bergman, *Phys. Rev. Lett.* **91**, 227402 (2003)

- Introduction: Plasmonics and Nano-confinement of Optical Energy
- Nanoplasmonic Resonances and their Frequencies (Colors)
- Localized Surface Plasmons and Plasmonic Hot Spots
- **Plasmonic Enhancement and Ultrafast Nature of Plasmonics**
- Adiabatic Nanofocusing
- Nanolenses
- Applications of Nanoplasmonics
- Sensing and Detection
- Plasmonic Nanoscopy
- Spaser as an Ultrafast Quantum Generator and Nanoamplifier

Enhancement factors for small nanoparticles (size $R < l_s \sim 25$ nm)

Plasmonic quality factor: $Q = \frac{\omega}{2\gamma} \approx \frac{-\text{Re } \epsilon_m}{\text{Im } \epsilon_m} \sim 10 - 100$

Radiative rate enhancement for dipole mode frequency: $\sim Q^2$

Excitation rate enhancement: $\sim Q^2$

SERS enhancement: $\sim Q^4$

The above-listed enhancement factors do not depend on size R

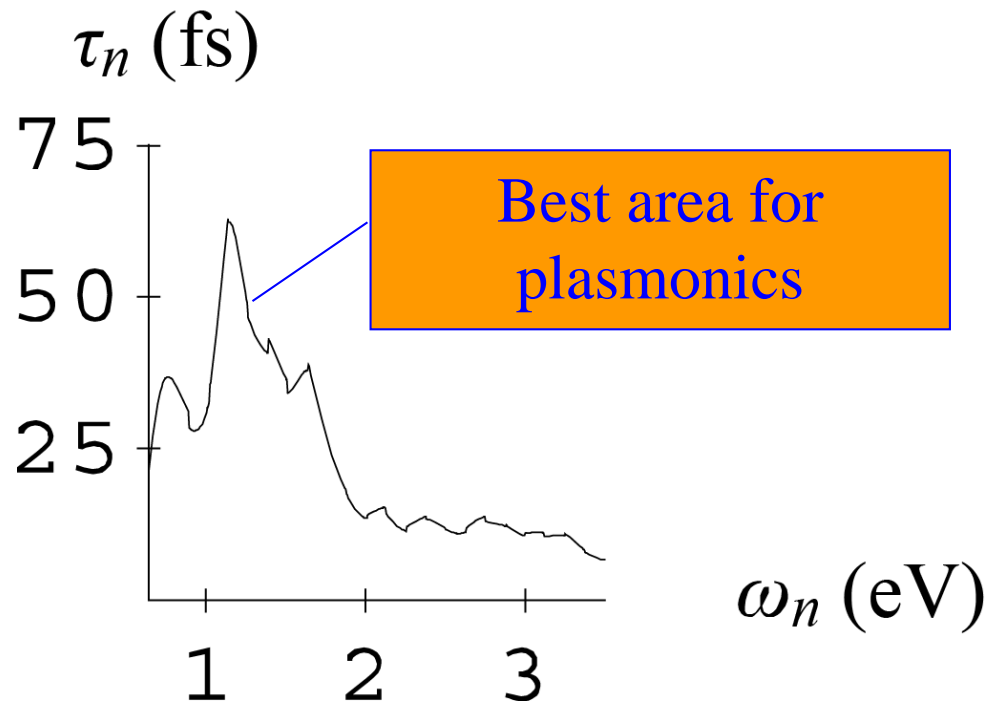
Emission rate of SPs into a mode: $\propto \frac{Q}{R^3}$

This relative to free photons: $\sim \frac{\lambda^3 Q}{R^3}$ (Purcell factor)

This enhancement factor is *inversely* proportional to R^3

This is of fundamental importance for spasers (plasmonic nanolasers)

Nanoplasmonics is intrinsically ultrafast:



Surface plasmon relaxation times are in
~10-100 fs range

Spectrally, surface plasmon resonances in complex systems occupy a very wide frequency band; for gold and silver:

$$\Delta\omega \approx \omega_p / \sqrt{2} \approx 4 \text{ eV}$$

Including aluminum with plasmon responses in the ultraviolet, this spectral width increases to ~10 eV.

Corresponding rise time of plasmonic responses ~ 100 as

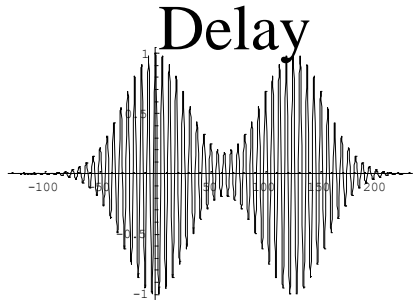
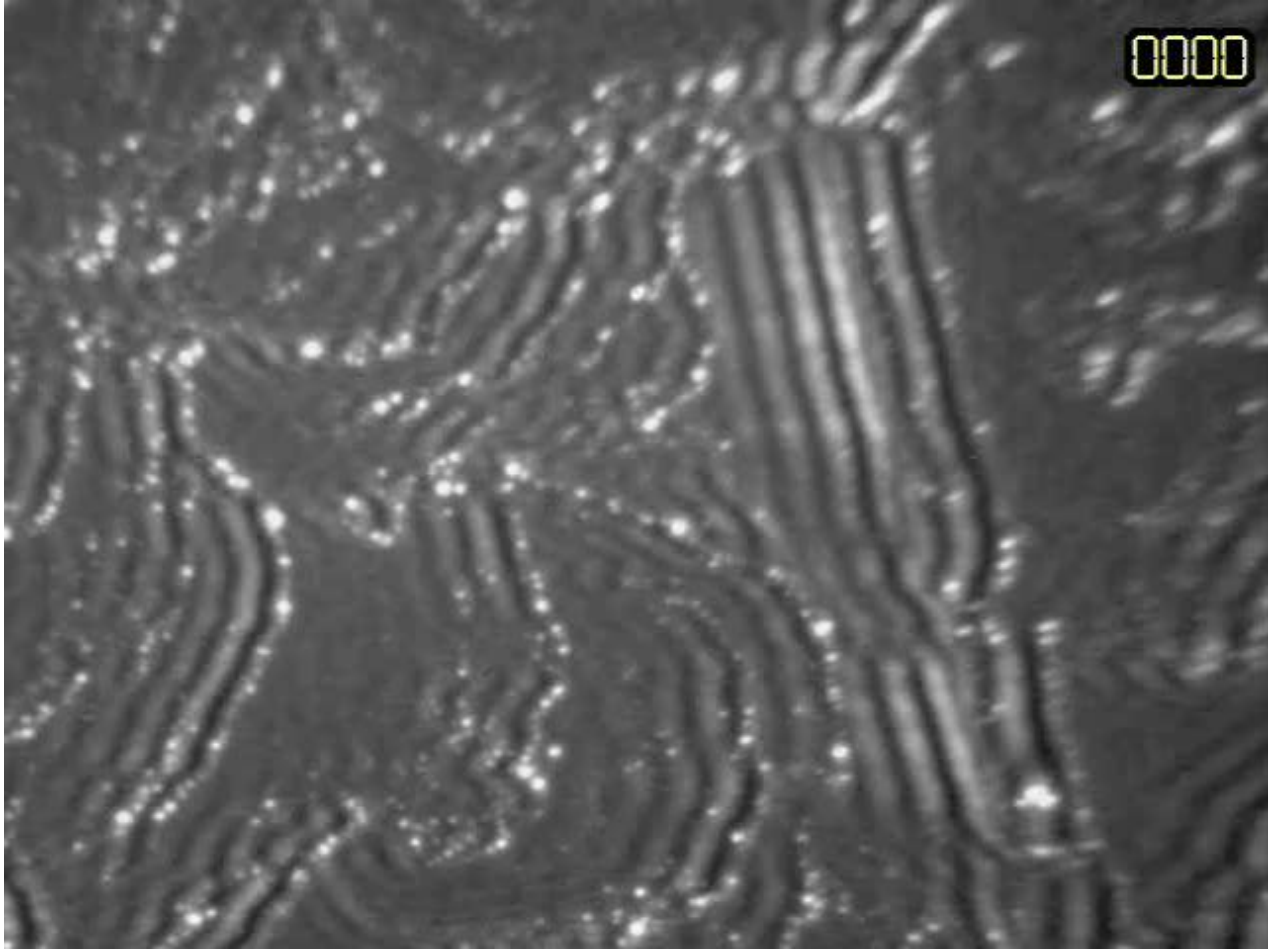
A. Kubo, K. Onda, H. Petek, Z. Sun, Y. S. Jung, and H. K. Kim, *Femtosecond Imaging of Surface Plasmon Dynamics in a Nanostructured Silver Film*, Nano Lett. 5, 1123 (2005).

PEEM Image as a Function of Delay (250 as per frame)

200 nm
↔

30 femtoseconds from life of a nanoplasmonic systems

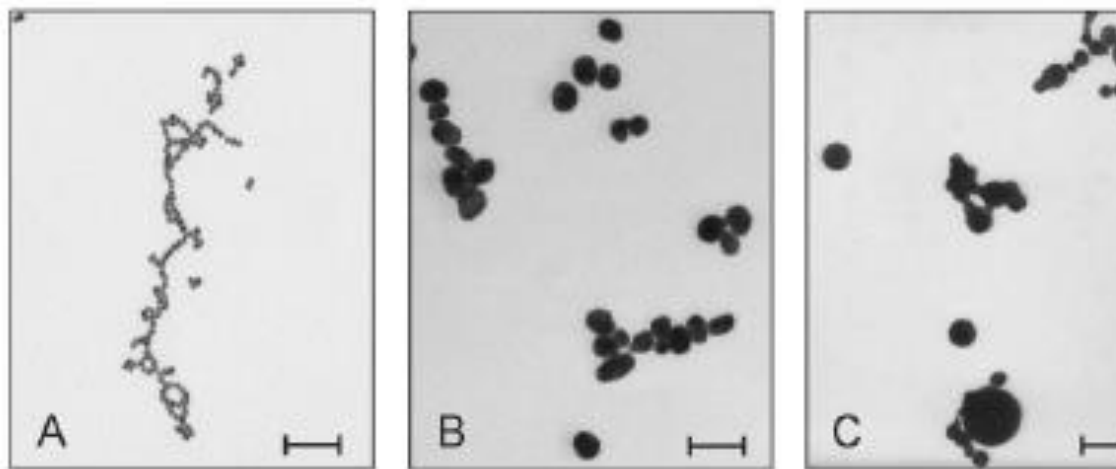
Localized SP hot spots are deeply subwavelength as seen in PEEM (photoemission electron microscope)



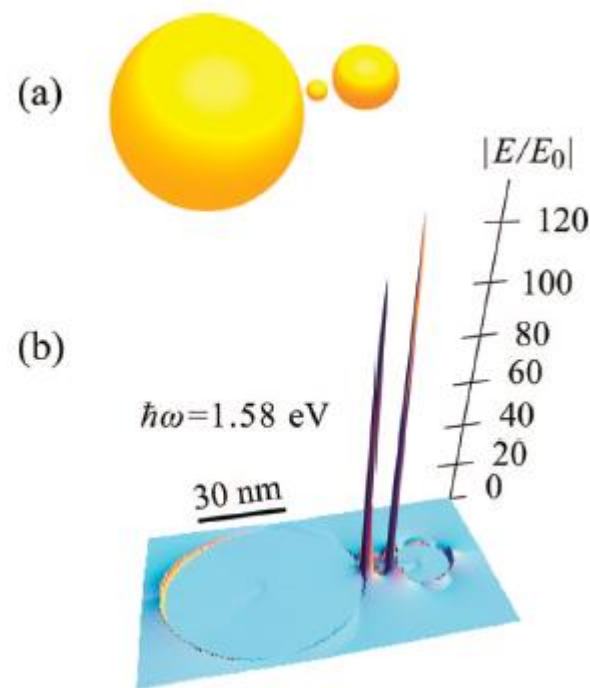
Different types of aggregates of gold nanospheres

Gold Nanolenses Generated by Laser Ablation-Efficient Enhancing Structure for Surface Enhanced Raman Scattering Analytics and Sensing

Janina Kneipp,^{*,†,‡} Xiangting Li,[§] Margaret Sherwood,[†] Ulrich Panne,[‡] Harald Kneipp,[†] Mark I. Stockman,[§] and Katrin Kneipp^{†,||}



Scale bar: 100 nm



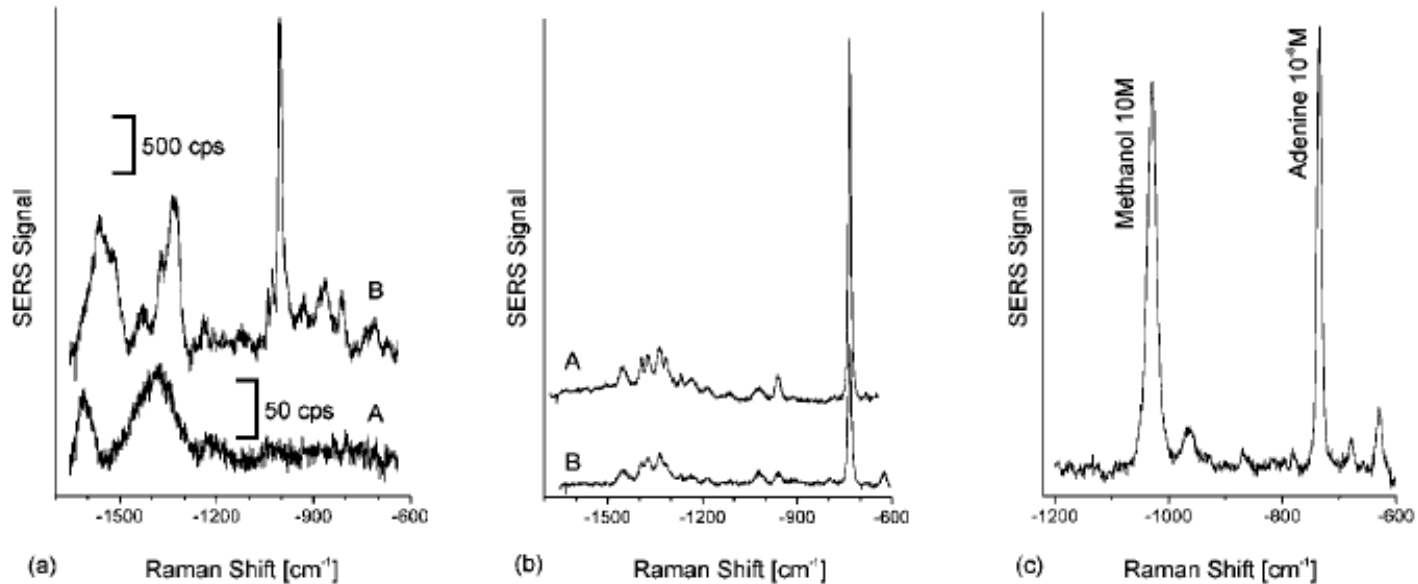


Figure 3. Comparison of SERS using gold nanolenses made by ablation and chemically prepared nanoaggregates as enhancing nanostructures. (a) Raman spectra measured from aqueous solutions of gold nanoaggregates without any analyte to compare background signals. The chemically prepared gold nanoparticles (spectrum B) display surface enhanced Raman lines, resulting from impurities introduced during the preparation process of this particular batch of colloids, such as the line at ~ 1000 cm^{-1} . The bands around 1500 cm^{-1} in the spectrum of the ablation nanoaggregates can be assigned to carbonate complexes.¹⁸ Spectra were measured at 50 mW at 785 nm excitation in 10 s (spectrum A) and 1 s (spectrum B) collection times. Abbreviation: cps, counts per second. (b) SERS signals of adenine measured in solutions of ablation aggregates (spectrum A) and chemically prepared nanoaggregates (spectrum B) using 10 mW at 785 nm excitation. (c) Comparison of the Raman signal of 10^{-8} M adenine and 10 M methanol measured in aqueous solutions of nanoaggregates.

Self-Similar Gold-Nanoparticle Antennas for a Cascaded Enhancement of the Optical Field

Christiane Höppener,^{1,2} Zachary J. Lapin,¹ Palash Bharadwaj,¹ and Lukas Novotny^{1,*}

¹*Institute of Optics, University of Rochester, Rochester, New York 14627, USA*

²*Institute of Physics, University of Münster, 48149 Münster, Germany*

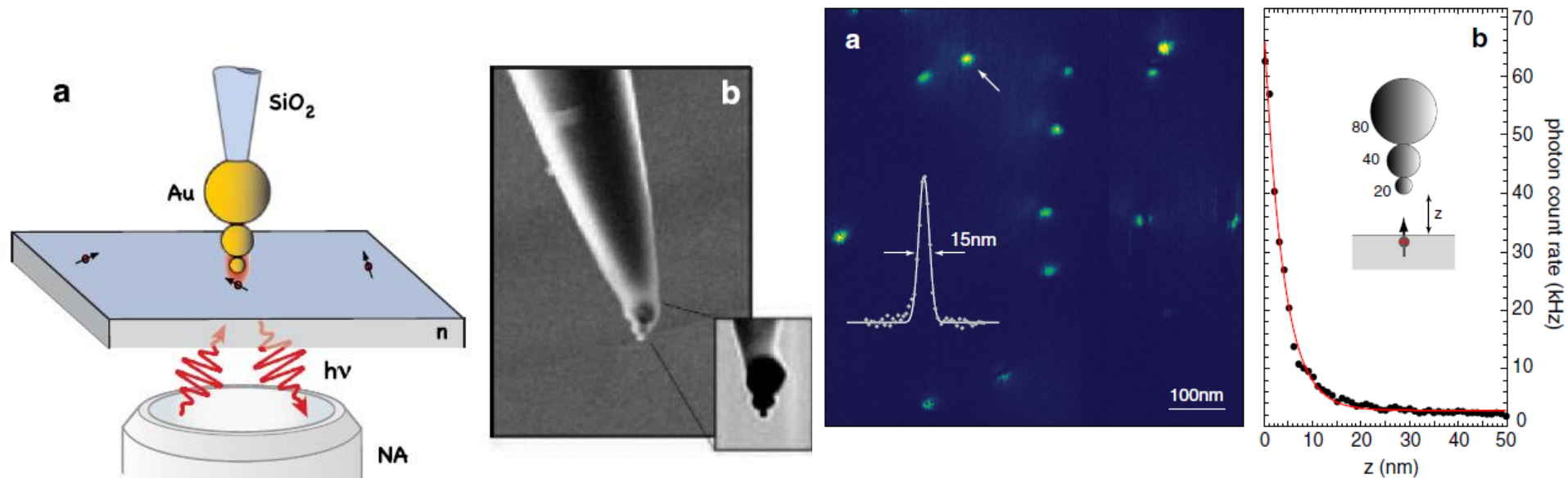


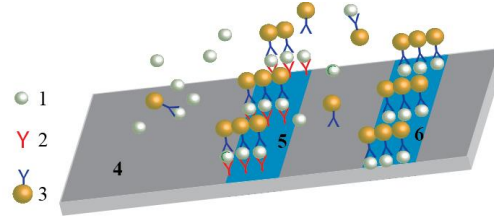
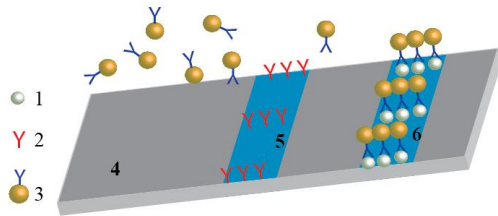
FIG. 4 (color online). Excitation of single-molecule fluorescence with a trimer antenna consisting of 80, 40, and 20 nm gold nanoparticles. (a) Fluorescence image of the single-molecule sample. Inset: Line cut through the single fluorescence spot marked by the arrow. (b) Fluorescence from a single z -oriented molecule recorded as a function of distance from a trimer antenna. The steep rise of fluorescence counts for separations smaller than 15 nm is due to strong field localization along the z axis at the apex of the trimer antenna.

- Introduction: Plasmonics and Nano-confinement of Optical Energy
- Nanoplasmonic Resonances and their Frequencies (Colors)
- Localized Surface Plasmons and Plasmonic Hot Spots
- Plasmonic Enhancement and Ultrafast Nature of Plasmonics
- Nanolenses
- **Applications of Nanoplasmonics**
- **Sensing and Detection**
- Plasmonic Nanoscopy
- Spaser as an Ultrafast Quantum Generator and Nanoamplifier: Introduction
- Spaser as an Ultrafast Quantum Generator and Nanoamplifier: Theory
- Spaser as an Ultrafast Quantum Generator and Nanoamplifier: Experiment

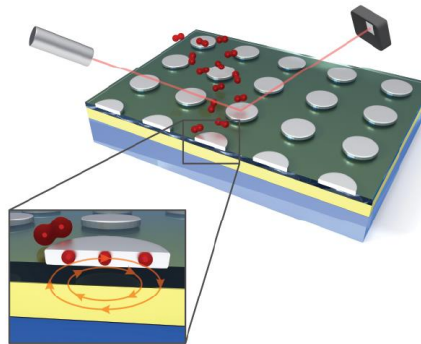
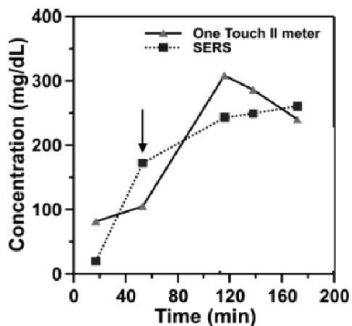
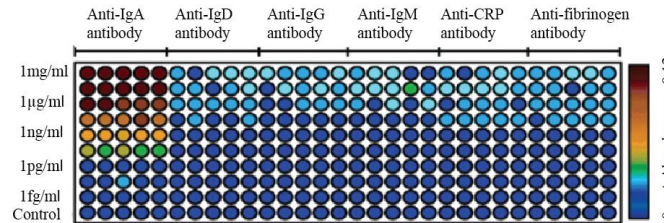
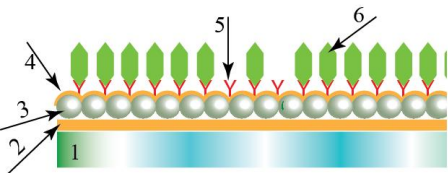
Sensing and Detection with Localized Surface Plasmons



Immunochemical assay with immunotargeted gold nanosphere suspension. Detection of: hCG (human chorionic gonadotropin) -- Home pregnancy test; PSA (prostate-specific antigen) -- Prostate cancer ; troponin -- heart attack test; HIV/AIDS (trials)

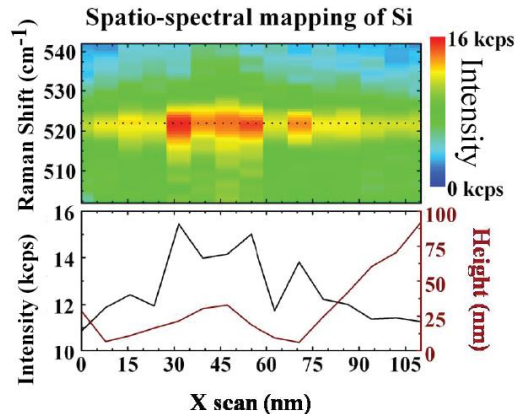
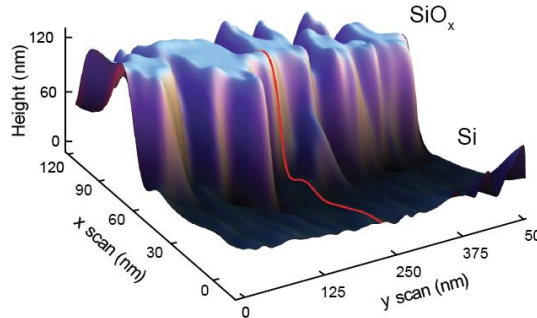
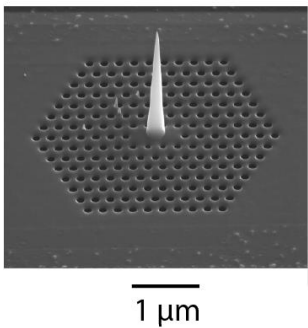
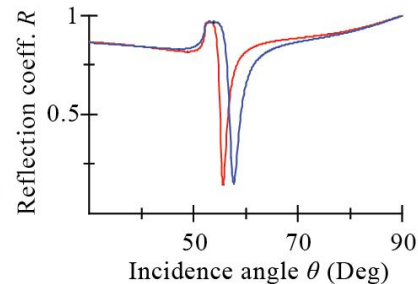
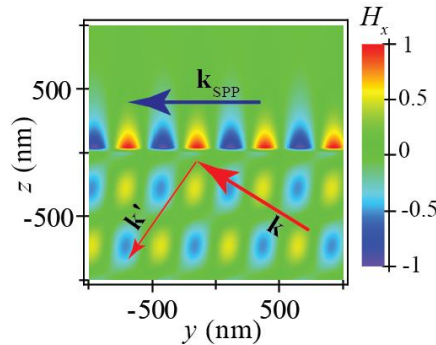
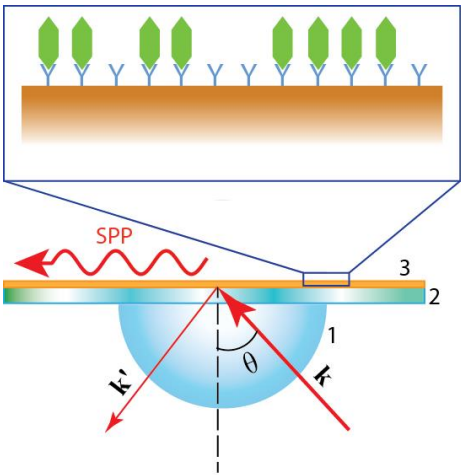


Immunoassay with immobilized immunotargeted gold nanospheres. T. Endo et al., *Multiple Label-Free Detection of Antigen-Antibody Reaction Using Localized Surface Plasmon ... Anal. Chem.* **78**, 6465-6475 (2006)



Left: Glucose in vivo monitoring using SERS from immobilized functionalized gold nanospheres. J. N. Anker, et al., *Biosensing with Plasmonic Nanosensors*, *Nat. Mater.* **7**, 442-453 (2008).
Right: Palladium-nanocylinder hydrogen sensor for hydrogen energy applications. H. Giessen et al.

Surface Plasmon Polariton Sensors



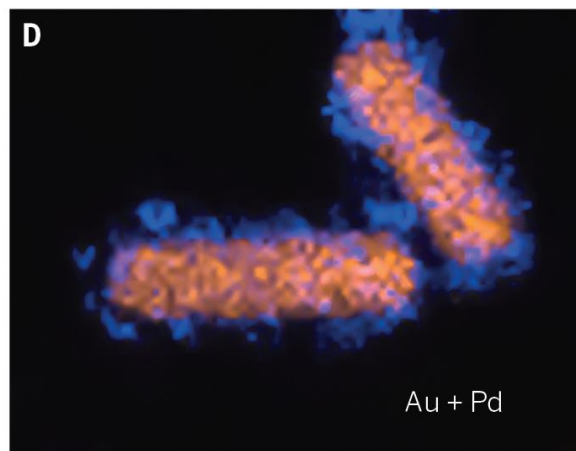
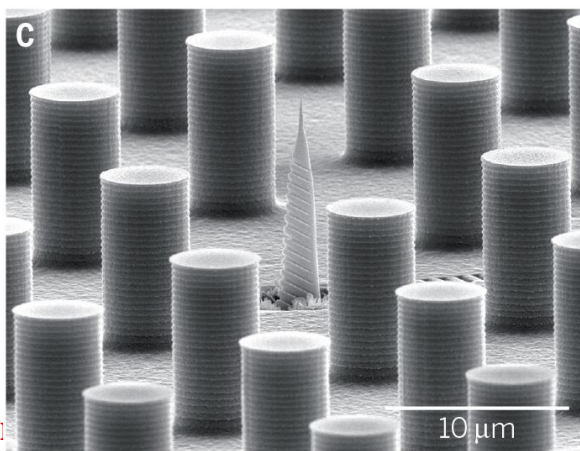
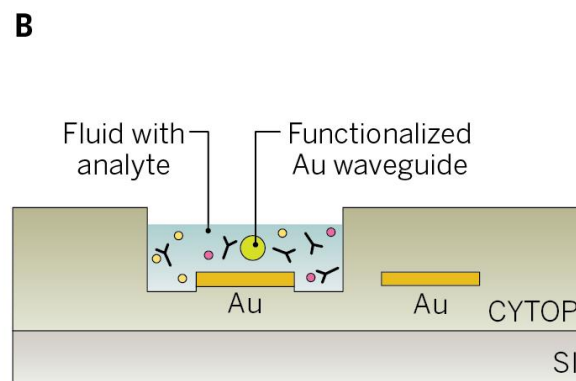
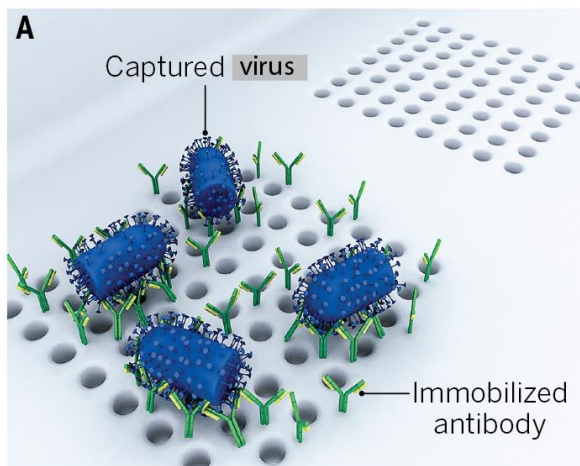
Surface plasmon polariton sensor based on Kretschmann geometry. Sensitivity $\sim 10^3 - 10^4$ large molecules. See, e.g., <http://www.biacore.com/>



Surface plasmon polariton SERS sensor and NSOM based on adiabatic concentration. Sensitivity ~ 100 molecules. F. De Angelis et al, *Nanoscale Chemical Mapping Using Three-Dimensional Adiabatic Compression of SPPs*. Nature Nanotechnology **5**, 67-72 (2009).

M. I. Stockman, *Nanoplasmonic Sensing and Detection*, Science **348**, 287-288 (2015).

Capture and detection

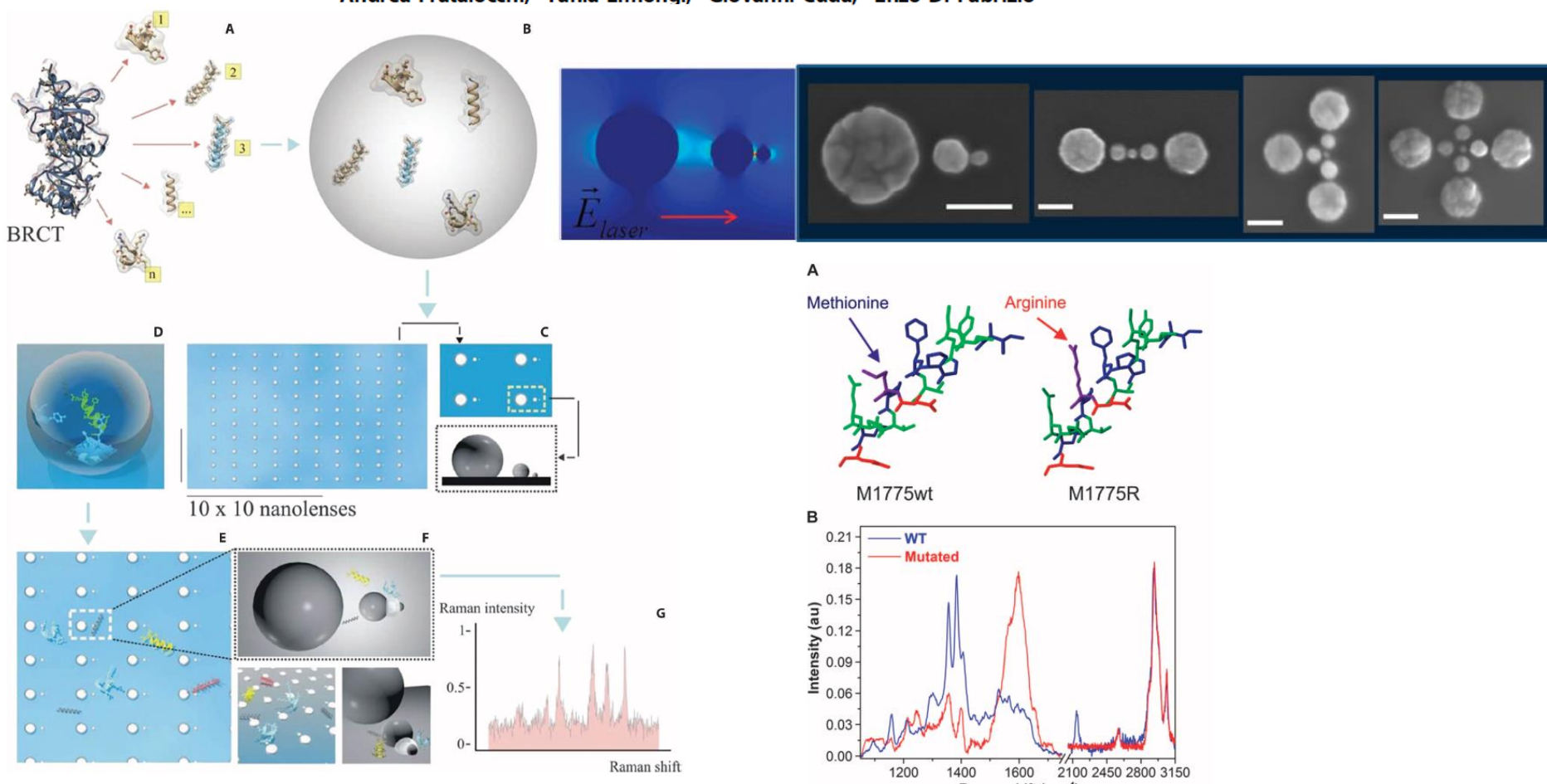


OPTICS

Detection of single amino acid mutation in human breast cancer by disordered plasmonic self-similar chain

Maria Laura Coluccio,¹ Francesco Gentile,^{1,2} Gobind Das,³ Annalisa Nicastrì,¹ Angela Mena Perri,¹ Patrizio Candeloro,¹ Gerardo Perozziello,¹ Remo Proietti Zaccaria,⁴ Juan Sebastian Toter Gongora,⁵ Salma Alrasheed,³ Andrea Fratolocchi,⁵ Tania Limonqi,³ Giovanni Cuda,¹ Enzo Di Fabrizio^{1,3*}

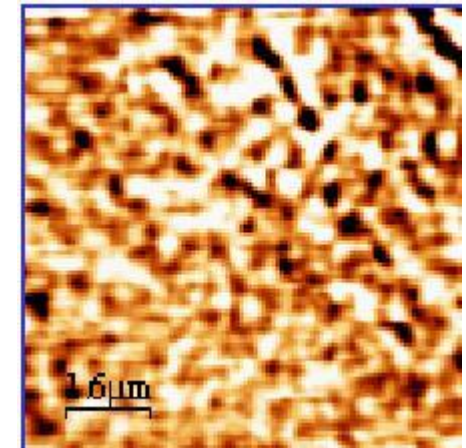
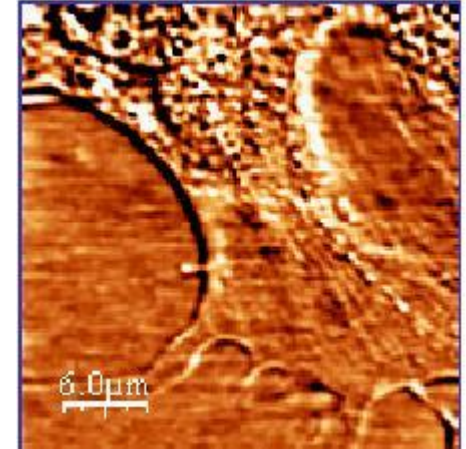
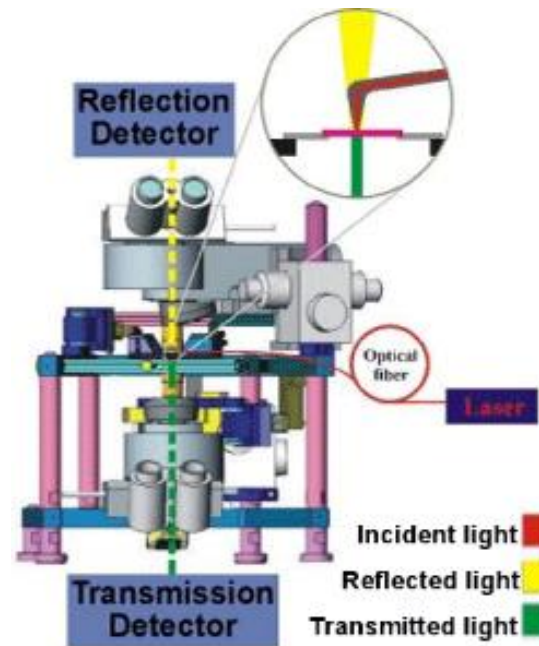
2015 © The Authors, some rights reserved; exclusive licensee American Association for the Advancement of Science. Distributed under a Creative Commons Attribution NonCommercial License 4.0 (CC BY-NC). 10.1126/sciadv.1500487



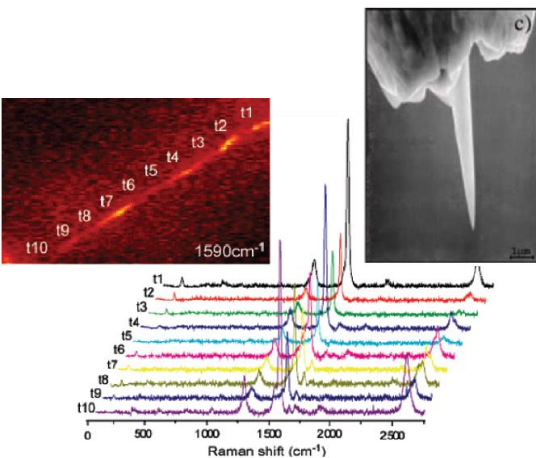
- Introduction: Plasmonics and Nano-confinement of Optical Energy
- Nanoplasmonic Resonances and their Frequencies (Colors)
- Localized Surface Plasmons and Plasmonic Hot Spots
- Plasmonic Enhancement and Ultrafast Nature of Plasmonics
- **Applications of Nanoplasmonics**
- Sensing and Detection
- **Plasmonic Nanoscopy**
- Spaser as an Ultrafast Quantum Generator and Nanoamplifier: Introduction
- Spaser as an Ultrafast Quantum Generator and Nanoamplifier: Theory
- Spaser as an Ultrafast Quantum Generator and Nanoamplifier: Experiment

Plasmonic Nanoscopy

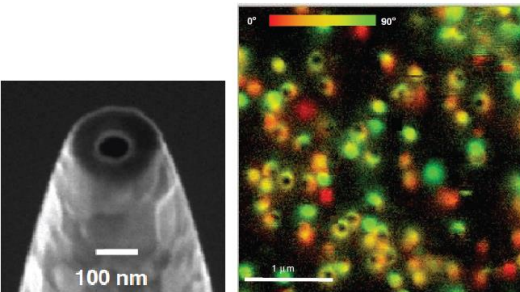
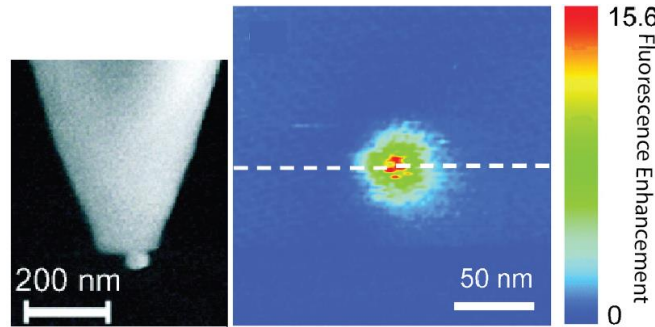
NSOM images of healthy human dermal fibroblasts in liquid obtained in transmission mode with a Nanonics cantilevered tip with a gold nanosphere (A. Lewis et al.)



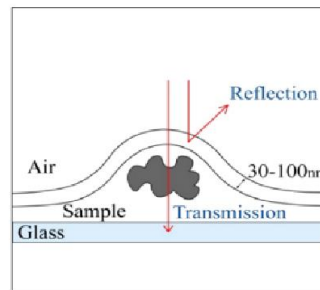
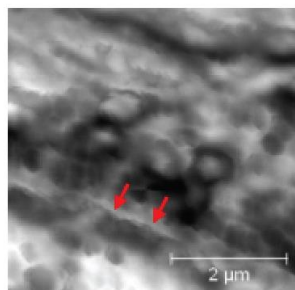
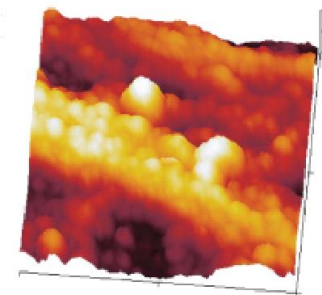
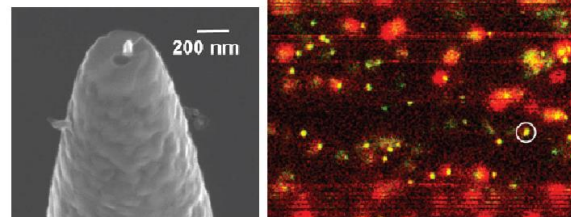
Plasmonic Nanoscopy



Left: Chemical vision: SERS image and spectra of a single-wall carbon nanotube obtained with a FIB-fabricated silver tip. L. Novotny and S. J. Stranick, *Annual Rev. Phys. Chem.* **57**, 303-331 (2006)
Right: Nanosphere probe and image of fluorescence enhancement of a single dye molecule. H. Eghlidi et al., *Nano Lett.* **9**, 4007-4011 (2009)



Left: Metallized tapered fiber probe and NSOM image of a single fluorescent molecules with polarization resolution.
Right: Nanoantenna-on-fiber probe and NSOM image of a single fluorescent molecules with polarization resolution. T. H. Taminiou, F. B. Segerink, R. J. Moerland, L. Kuipers, and N. F. van Hulst, *Journal of Optics a-Pure and Applied Optics* **9**, S315-S321 (2007)



Imaging of living cells in culture with a tapered fiber NSOM. Left: Topology, Center: NSOM image, Right: Schematic. E. Trevisan, E. Fabbretti, N. Medic, B. Troian, S. Prato, F. Vita, G. Zabcuchi, and M. Zwyer, *Novel Approaches for Scanning near-Field Optical Microscopy Imaging of Oligodendrocytes in Culture*, *Neuroimage* **49**, 517-524 (2010)

- Introduction: Plasmonics and Nano-confinement of Optical Energy
- Nanoplasmonic Resonances and their Frequencies (Colors)
- Localized Surface Plasmons and Plasmonic Hot Spots
- Plasmonic Enhancement and Ultrafast Nature of Plasmonics
- Nanolenses
- Applications of Nanoplasmonics
- Sensing and Detection
- Plasmonic Nanoscopy
- **Spaser as an Ultrafast Quantum Generator and Nanoamplifier: Introduction**
- Spaser as an Ultrafast Quantum Generator and Nanoamplifier: Theory
- Spaser as an Ultrafast Quantum Generator and Nanoamplifier: Experiment

Dawn of the new bold era: seminal first paper on laser (originally “optical maser” then laser)

[nature.com](#) | [about npg](#) | news@nature.com | [naturejobs](#) | [natureevents](#) | [help](#) | [site index](#) |

nature

[my account](#) | [e-alerts](#) | [subscribe](#) | [register](#)

SEARCH JOURNAL

Go

Thursday 12 September 2013

[Journal Home](#)
[Current Issue](#)
[AOP](#)
[Archive](#)

THIS ARTICLE

[Download PDF](#)
[References](#)

[Export citation](#)
[Export references](#)

[Send to a friend](#)

More articles like this

[Table of Contents](#)
< [Previous](#) | [Next](#) >

letters to nature

Nature 187, 493 - 494 (06 August 1960); doi:10.1038/187493a0

Stimulated Optical Radiation in Ruby

T. H. MAIMAN

Hughes Research Laboratories, A Division of Hughes Aircraft Co., Malibu, California.

Schawlow and Townes¹ have proposed a technique for the generation of very monochromatic radiation in the infra-red optical region of the spectrum using an alkali vapour as the active medium. Javan² and Sanders³ have discussed proposals involving electron-excited gaseous systems. In this laboratory an optical pumping technique has been successfully applied to a fluorescent solid resulting in the attainment of negative temperatures and stimulated optical emission at a wave-length of 6943 Å. ; the active material used was ruby (chromium in corundum).

1. Schawlow, A. L. , and Townes, C. H. , *Phys. Rev.*, **112**, 1940 (1958). | [Article](#) | [ISI](#) | [ChemPort](#) |
2. Javan, A. , *Phys. Rev. Letters*, **3**, 87 (1959). | [Article](#) | [ISI](#) |
3. Sanders, J. H. , *Phys. Rev. Letters*, **3**, 86 (1959). | [Article](#) | [ISI](#) | [ChemPort](#) |
4. Maiman, T. H. , *Phys. Rev. Letters*, **4**, 564 (1960). | [Article](#) | [ISI](#) |

Surface Plasmon Amplification by Stimulated Emission of Radiation: Quantum Generation of Coherent Surface Plasmons in Nanosystems

David J. Bergman^{1,*} and Mark I. Stockman^{2,†}

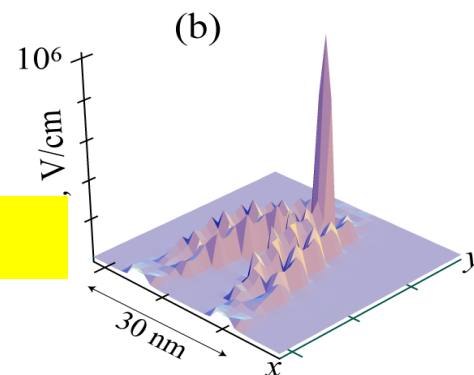
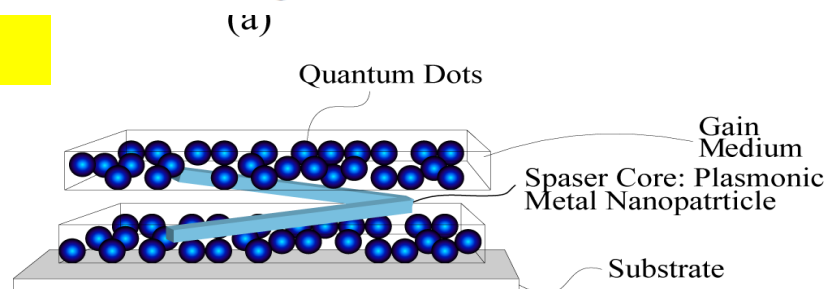
¹*School of Physics and Astronomy, Raymond and Beverly Sackler Faculty of Exact Sciences, Tel Aviv University, Tel Aviv, 69978, Israel*

²*Department of Physics and Astronomy, Georgia State University, Atlanta, Georgia 30303*

(Received 15 September 2002; published 14 January 2003)

We make a step towards quantum nanoplasmonics: surface plasmon fields of a nanosystem are quantized and their stimulated emission is considered. We introduce a quantum generator for surface plasmon quanta and consider the phenomenon of surface plasmon amplification by stimulated emission of radiation (spaser). Spaser generates temporally coherent high-intensity fields of selected surface plasmon modes that can be strongly localized on the nanoscale, including dark modes that do not couple to far-zone electromagnetic fields. Applications and related phenomena are discussed.

The original spaser proposal

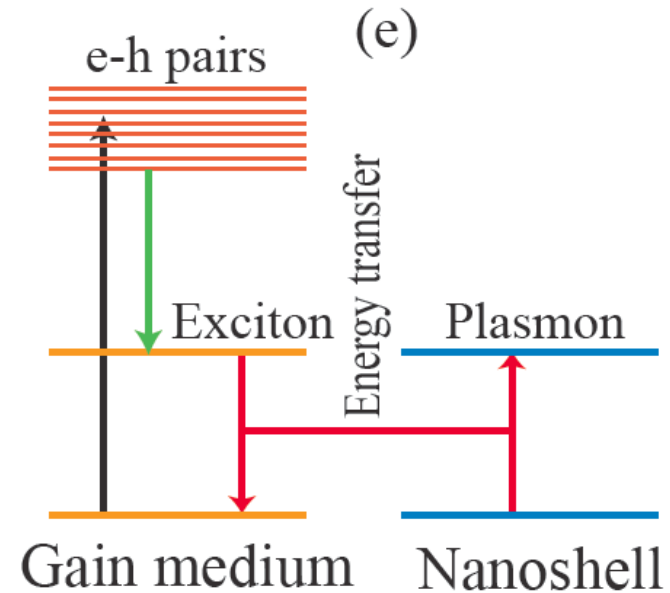
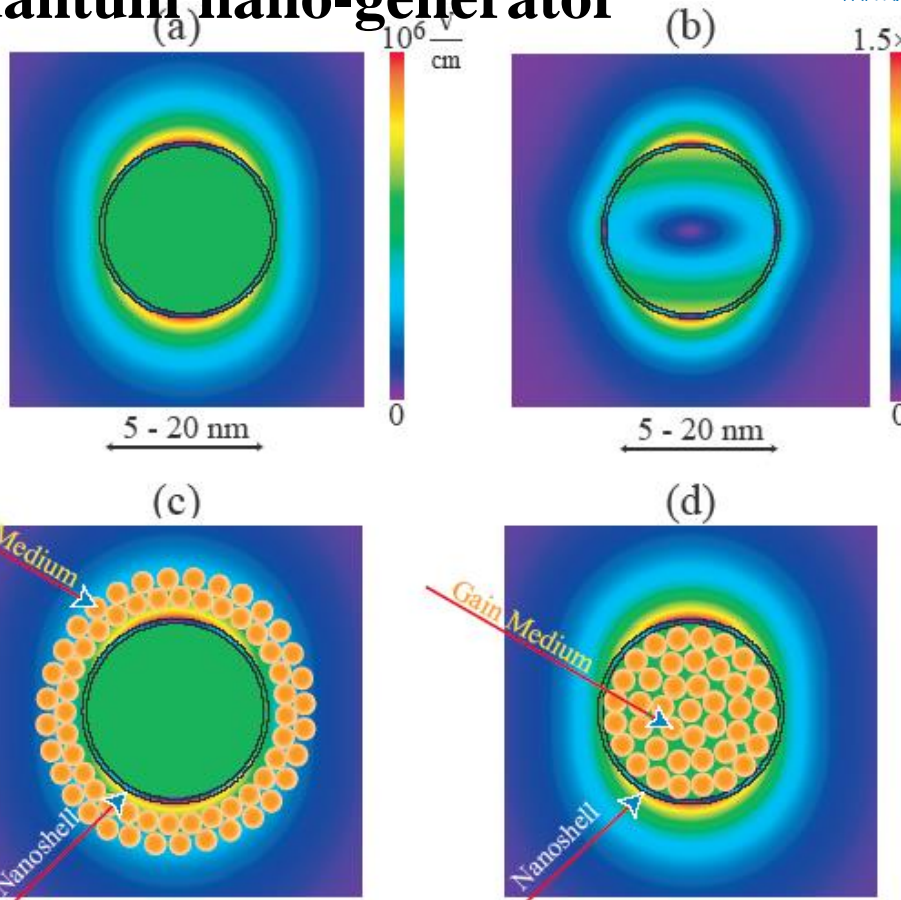


Spaser field per one plasmon in the core

Spaser is the ultimately smallest quantum nano-generator

For small nanoparticles, radiative loss is negligible.

Spaser is fully scalable



D. J. Bergman and M. I. Stockman, *Surface Plasmon Amplification by Stimulated Emission of Radiation: Quantum Generation of Coherent Surface Plasmons in Nanosystems*, Phys. Rev. Lett. **90**, 027402-1-4 (2003).

- Introduction: Plasmonics and Nano-confinement of Optical Energy
- Nanoplasmonic Resonances and their Frequencies (Colors)
- Localized Surface Plasmons and Plasmonic Hot Spots
- Plasmonic Enhancement and Ultrafast Nature of Plasmonics
- Nanolenses
- Applications of Nanoplasmonics
- Sensing and Detection
- Plasmonic Nanoscopy
- Spaser as an Ultrafast Quantum Generator and Nanoamplifier: Introduction
- **Spaser as an Ultrafast Quantum Generator and Nanoamplifier: Theory**
- Spaser as an Ultrafast Quantum Generator and Nanoamplifier: Experiment

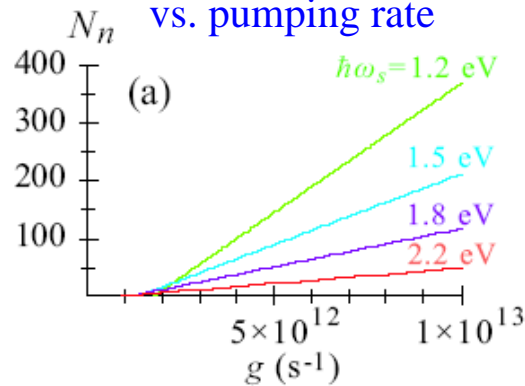
Stationary (CW) spaser regime

This quasilinear dependence of the number of plasmons per mode $N_n(g)$ is a result of the very strong feedback in spaser due to the small modal volume

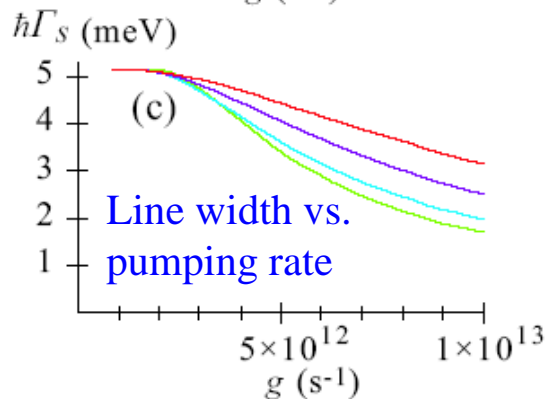
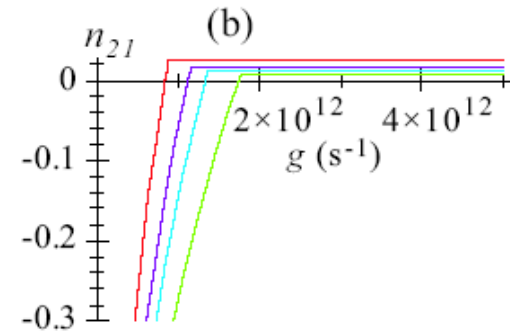
$$\Gamma_s \propto g^{-1}$$

[arXiv:0908.3559](https://arxiv.org/abs/0908.3559)
 Journal of Optics, **12**,
 024004-1-13 (2010).

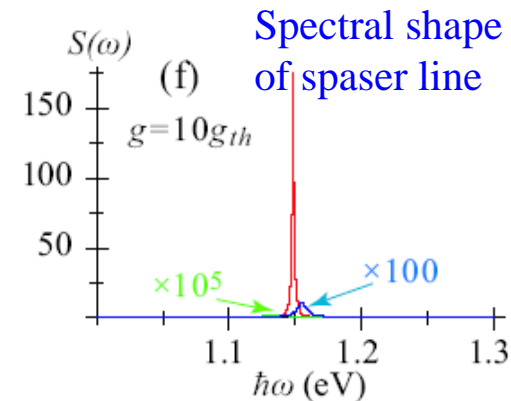
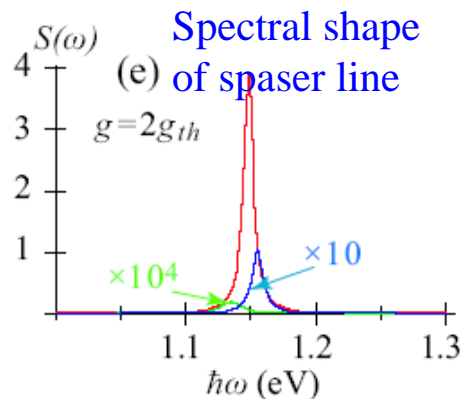
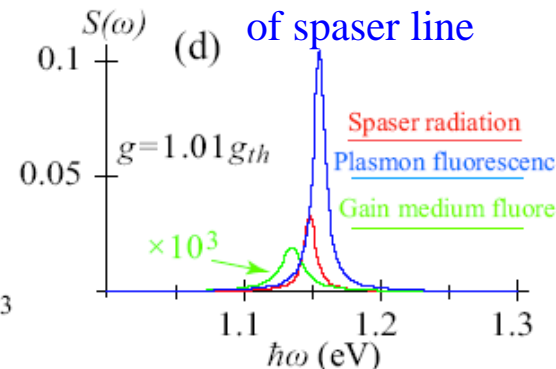
Plasmon number vs. pumping rate



Inversion vs. pumping rate

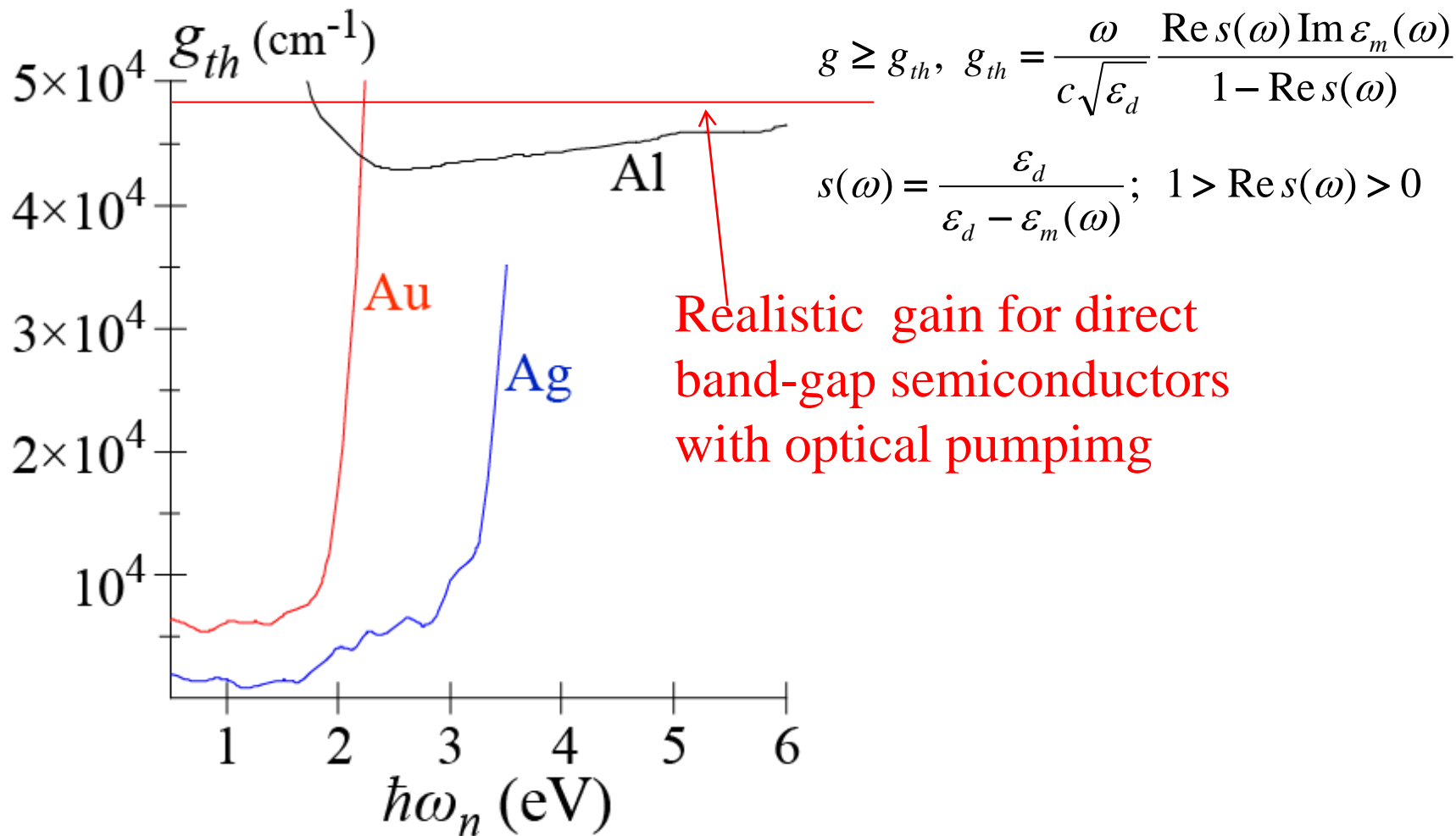


Spectral shape of spaser line



Gain of bulk medium required for spasing and for loss compensation by gain:

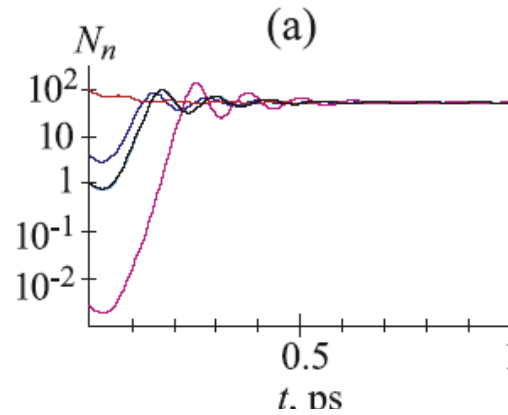
M. I. Stockman, *Spaser Action, Loss Compensation, and Stability in Plasmonic Systems with Gain*, Phys. Rev. Lett. **106**, 156802-1-4 (2011); Phil. Trans. R. Soc. A **369**, 3510 (2011).



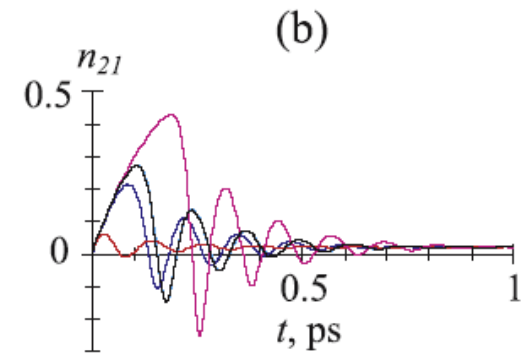
Amplification in Spaser without a Saturable Absorber

Stationary pumping

SP coherent population

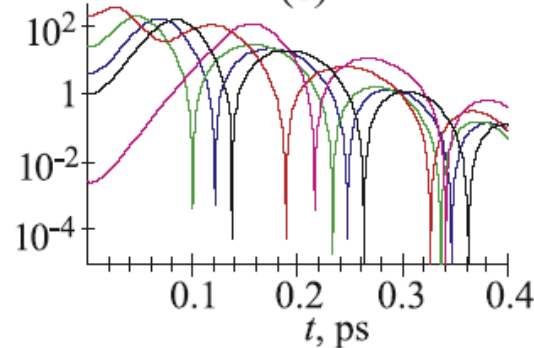


Population inversion

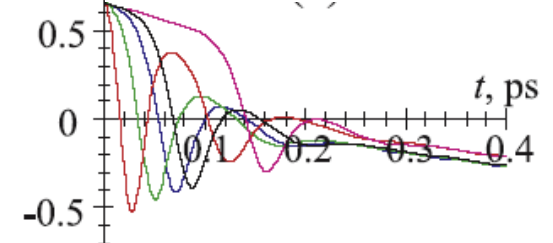


Pulse pumping

SP coherent population



Population inversion

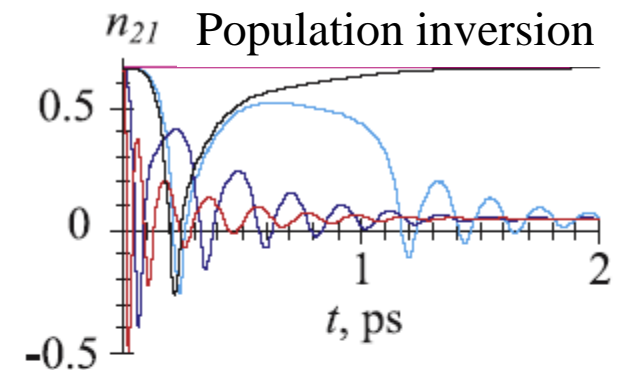
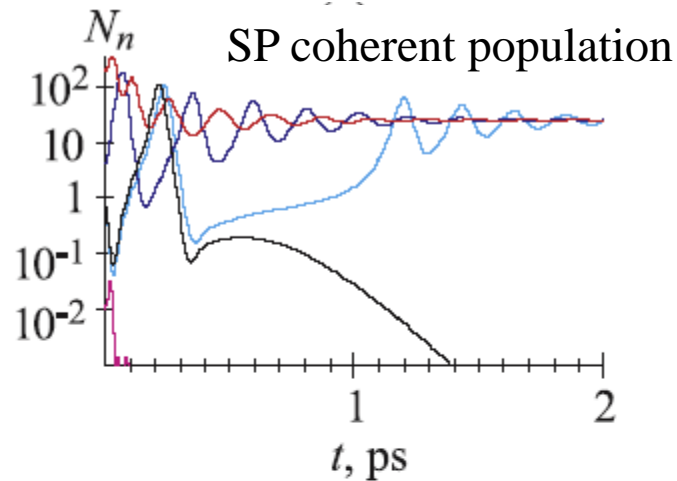


Bandwidth $\sim 10\text{-}100$ THz

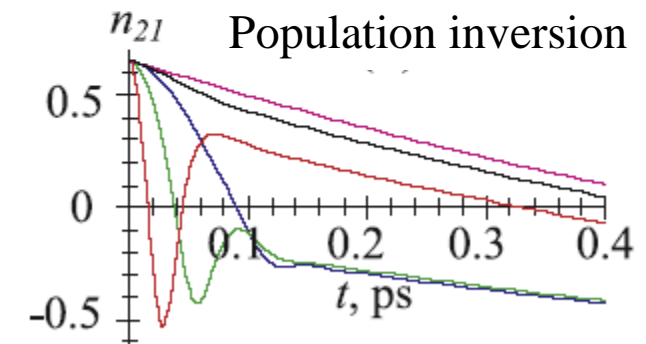
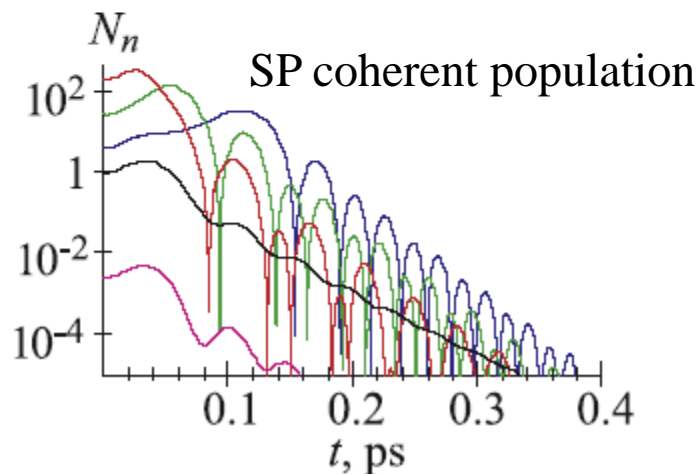
Very high resistance to ionizing radiation

Amplification in Spaser with a Saturable Absorber (1/3 of the gain chromophores)

Stationary pumping



Pulse pumping



- Introduction: Plasmonics and Nano-confinement of Optical Energy
- Nanoplasmonic Resonances and their Frequencies (Colors)
- Localized Surface Plasmons and Plasmonic Hot Spots
- Plasmonic Enhancement and Ultrafast Nature of Plasmonics
- Nanolenses
- Applications of Nanoplasmonics
- Sensing and Detection
- Plasmonic Nanoscopy
- Spaser as an Ultrafast Quantum Generator and Nanoamplifier: Introduction
- Spaser as an Ultrafast Quantum Generator and Nanoamplifier: Theory
- **Spaser as an Ultrafast Quantum Generator and Nanoamplifier: Experiment**

Demonstration of a spaser-based nanolaser

M. A. Noginov¹, G. Zhu¹, A. M. Belgrave¹, R. Bakker², V. M. Shalaev², E. E. Narimanov², S. Stout^{1,3}, E. Herz³, T. Suteewong³ & U. Wiesner³

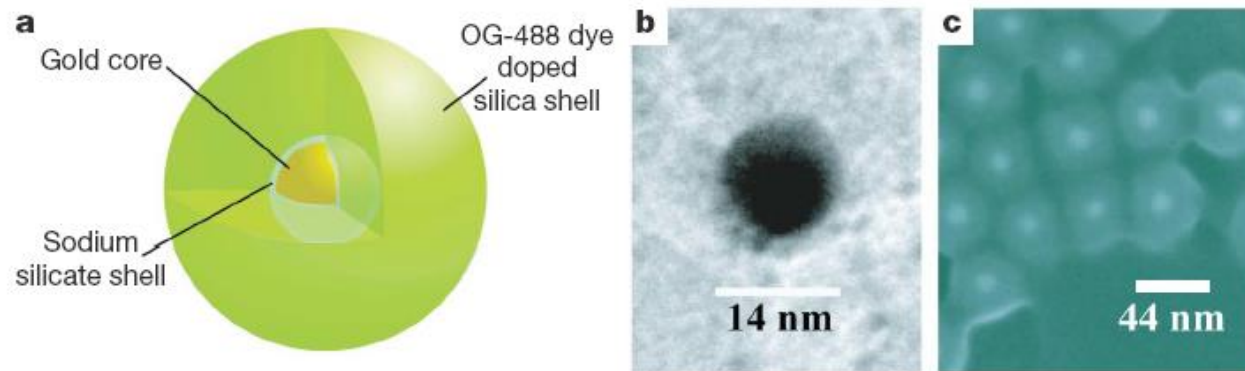


Figure 1 | Spaser design. **a**, Diagram of the hybrid nanoparticle architecture (not to scale), indicating dye molecules throughout the silica shell. **b**, Transmission electron microscope image of Au core. **c**, Scanning electron microscope image of Au/silica/dye core-shell nanoparticles. **d**, Spaser mode

(in false colour), with $\lambda = 515$ nm. The white circles represent the 14-nm Au cores. The false colour scheme is shown in the inset.

¹Center for Materials Research, Norfolk State University, Norfolk, Virginia 23504, USA. ²School of Electrical & Computer Engineering, Purdue University, West Lafayette, Indiana 47907, USA. ³Materials Science and Engineering Department, Cornell University, Ithaca, New York 14853, USA.

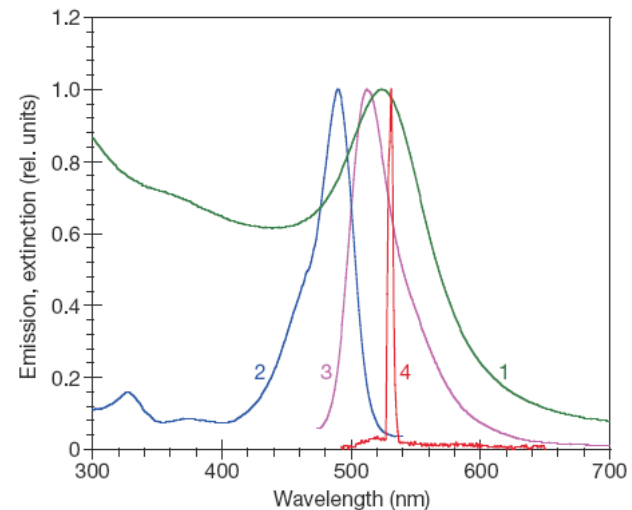


Figure 2 | Spectroscopic results. Normalized extinction (1), excitation (2), spontaneous emission (3), and stimulated emission (4) spectra of Au/silica/dye nanoparticles. The peak extinction cross-section of the nanoparticles is $1.1 \times 10^{-12} \text{ cm}^2$. The emission and excitation spectra were measured in a spectrofluorometer at low fluence.

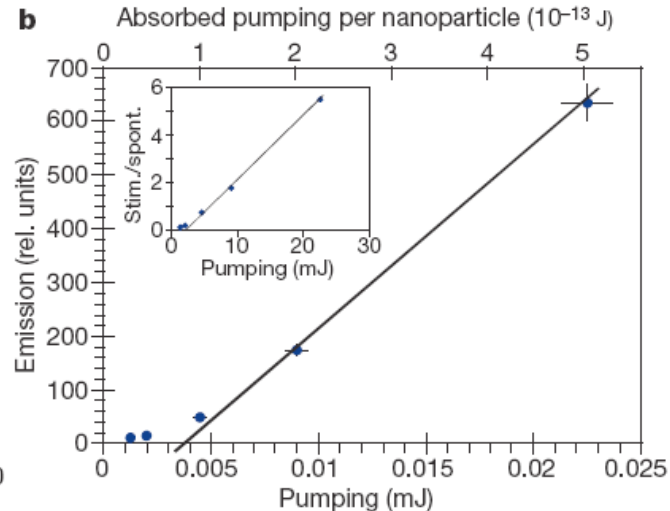
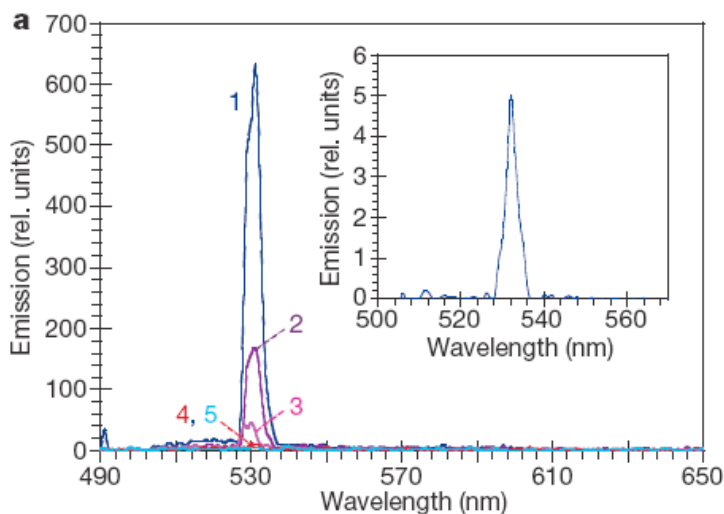


Figure 4 | Stimulated emission. **a**, Main panel, stimulated emission spectra of the nanoparticle sample pumped with 22.5 mJ (1), 9 mJ (2), 4.5 mJ (3), 2 mJ (4) and 1.25 mJ (5) 5-ns optical parametric oscillator pulses at $\lambda = 488 \text{ nm}$. **b**, Main panel, corresponding input-output curve (lower axis, total launched pumping energy; upper axis, absorbed pumping energy per nanoparticle); inset, ratio of the stimulated emission intensity (integrated between 526 nm and 537 nm) to the spontaneous emission background (integrated at $< 526 \text{ nm}$ and $> 537 \text{ nm}$).

by the noise of the photodetector and the instability of the pumping laser) do not exceed the size of the symbol. Inset of **a**, stimulated emission spectrum at more than 100-fold dilution of the sample. Inset of **b**, the ratio of the stimulated emission intensity (integrated between 526 nm and 537 nm) to the spontaneous emission background (integrated at $< 526 \text{ nm}$ and $> 537 \text{ nm}$).

Lasing in metal-insulator-metal sub-wavelength plasmonic waveguides

Martin T. Hill^{1*}, Milan Marell¹, Eunice S. P. Leong², Barry Smalbrugge¹, Youcai Zhu¹, Minghua Sun², Peter J. van Veldhoven¹, Erik Jan Geluk¹, Fouad Karouta¹, Yok-Siang Oei¹, Richard Nötzel¹, Cun-Zheng Ning², and Meint K. Smit¹

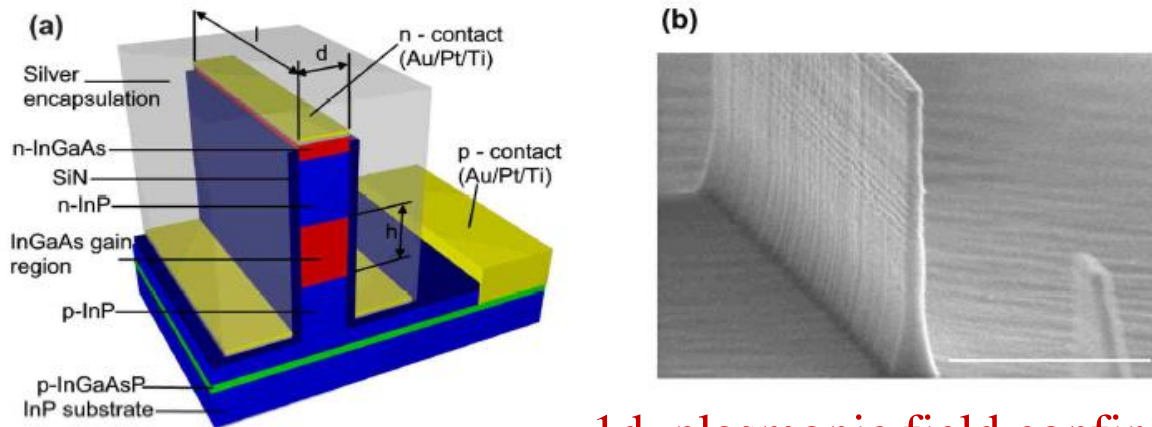
¹COBRA Research Institute, Technische Universiteit Eindhoven, Postbus 513, 5600 MB Eindhoven, The Netherlands

²Department of Electrical Engineering, Arizona State University, Tempe AZ 85287, USA

*m.t.hill@ieee.org

Received 14 Apr 2009; revised 8 Jun 2009; accepted 9 Jun 2009; published 18 Jun 2009

22 June 2009 / Vol. 17, No. 13 / OPTICS EXPRESS 11107



1d plasmonic field confinement

Fig. 1. Structure of cavity formed by a rectangular semiconductor pillar encapsulated in Silver. (a) Schematic showing the device layer structure. (b) Scanning electron microscope image showing the semiconductor core of one of the devices. The scale bar is 1 micron.

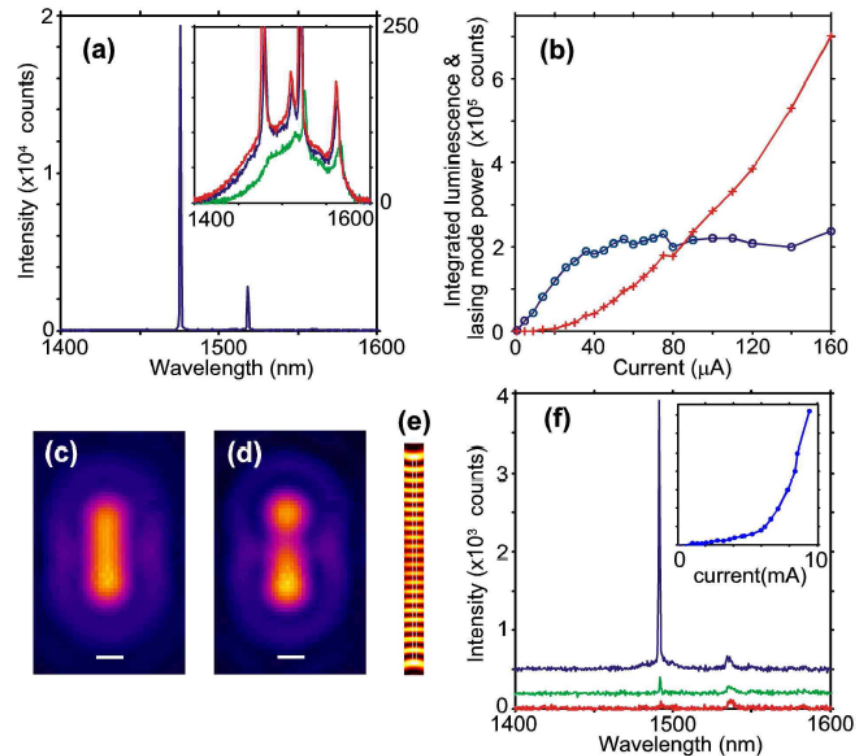
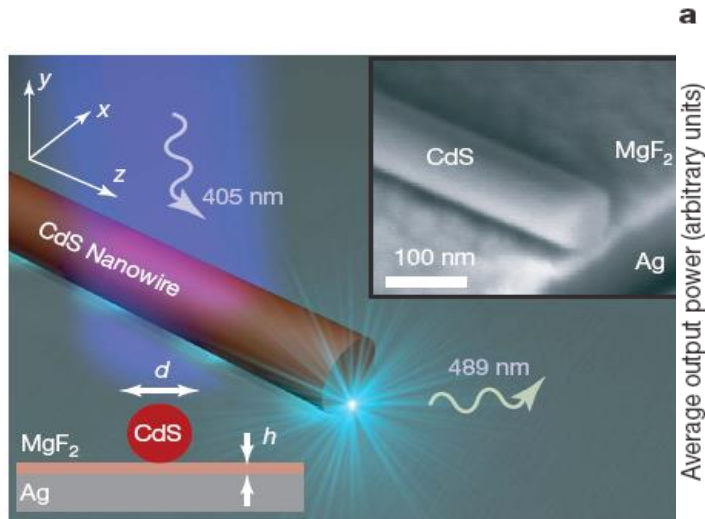


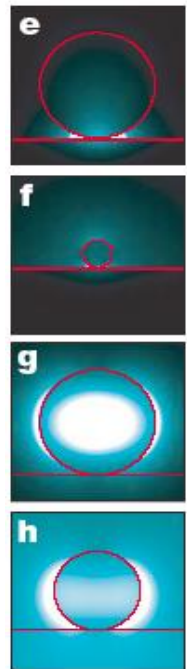
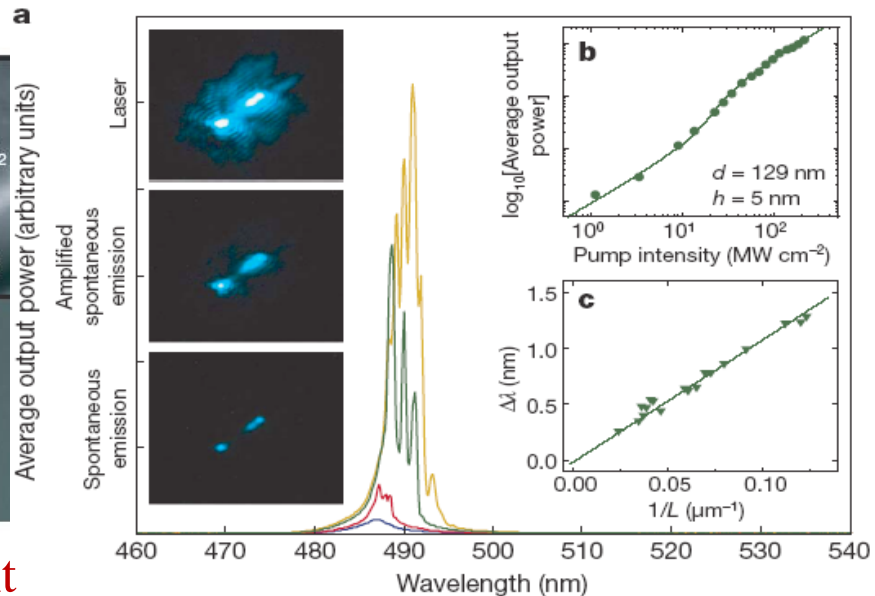
Fig. 2. Spectra and near field patterns showing lasing in devices. (a) Above threshold emission spectrum for 3 micron long device with semiconductor core width $d \sim 130\text{nm}$ ($\pm 20\text{nm}$), with pump current $180\ \mu\text{A}$ at 78K . Inset: emission spectra for 20 (green), 40 (blue) and 60 (red) μA , all at 78K . (b) Lasing mode light output (red crosses), integrated luminescence (blue circles), versus pump current for 78K . (c) Actual near field pattern (in x - y plane) for 6 micron ($d = 130\text{nm}$) device captured with $100\times$, 0.7 NA long working distance microscope objective and infrared camera, the scale bar is 2 micron, for below threshold $30\ \mu\text{A}$, and (d) above threshold $320\ \mu\text{A}$. (e) Simulated vertical (z) component of the Poynting vector taken at 0.7 microns below the pillar base, shows most emitted light at ends of device. (f) Spectra for a 6 micron long device with $d \sim 310\text{nm}$ at 298K , pulsed operation (28 ns wide pulses, 1MHz repetition). Spectra for peak currents of 5.2mA (red), 5.9mA (green) and 7.4mA (blue), (currents were estimated from the applied voltage pulse amplitude). The spectra for 5.9 and 7.4 mA are offset from 0 for clarity. Inset shows the total light collected by the spectrometer from the device for currents ranging from 0 to 10mA .

Plasmon lasers at deep subwavelength scale

Rupert F. Oulton^{1*}, Volker J. Sorger^{1*}, Thomas Zentgraf^{1*}, Ren-Min Ma³, Christopher Gladden¹, Lun Dai³, Guy Bartal¹ & Xiang Zhang^{1,2}



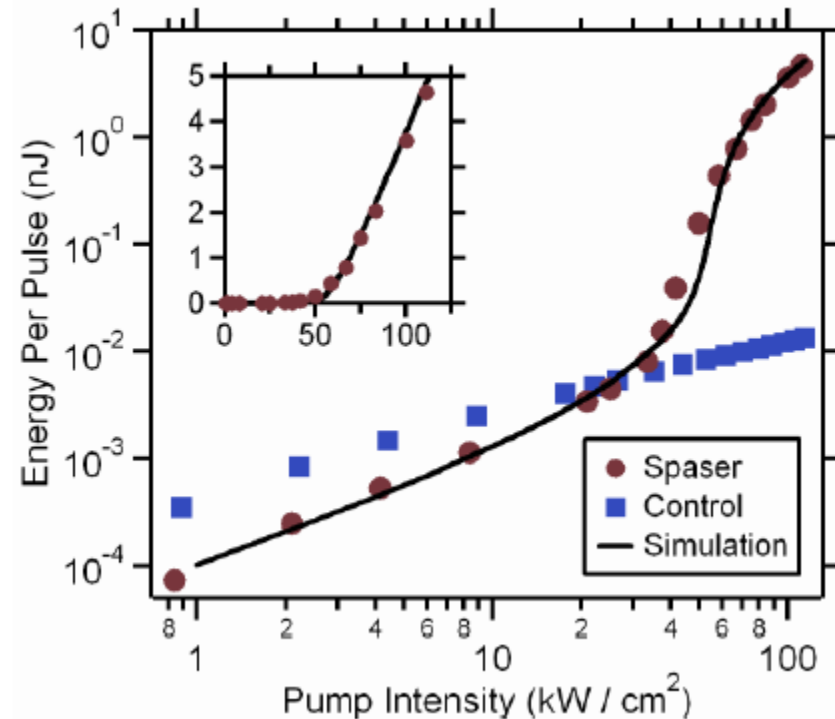
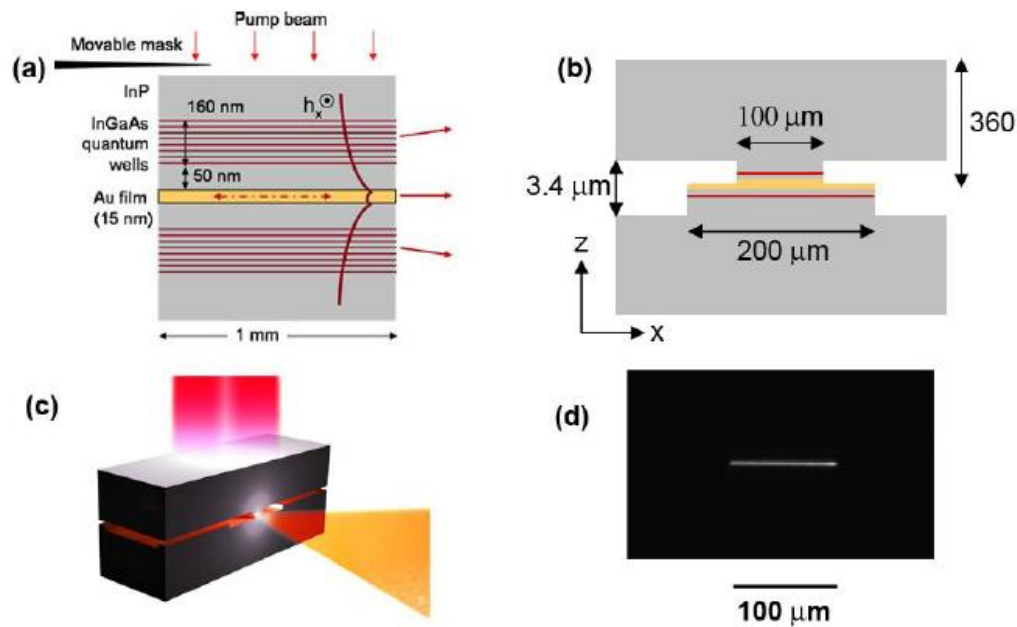
2d plasmonic field confinement



A room-temperature semiconductor spaser operating near 1.5 μm

R. A. Flynn,¹ C. S. Kim,¹ I. Vurgaftman,¹ M. Kim,¹ J. R. Meyer,¹ A. J. Mäkinen,¹
 K. Bussmann,² L. Cheng,³ F.-S. Choa,³ and J. P. Long^{4,*}

25 April 2011 / Vol. 19, No. 9 / OPTICS EXPRESS 8954



Plasmonic Nanolaser Using Epitaxially Grown Silver Film

Yu-Jung Lu,^{1*} Jisun Kim,^{2*} Hung-Ying Chen,¹ Chihhui Wu,² Nima Dabidian,² Charlotte E. Sanders,² Chun-Yuan Wang,¹ Ming-Yen Lu,³ Bo-Hong Li,⁴ Xianggang Qiu,⁴ Wen-Hao Chang,⁵ Lih-Juann Chen,³ Gennady Shvets,² Chih-Kang Shih,^{2†} Shangjr Gwo^{1†}

Having developed epitaxially grown, atomically smooth Ag films as a scalable plasmonic platform, we report a SPASER under CW operation with an ultralow lasing threshold at liquid nitrogen temperature and a mode volume well below the 3D diffraction limit. The device has

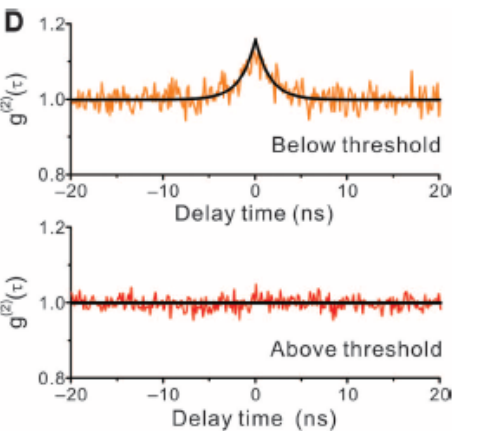
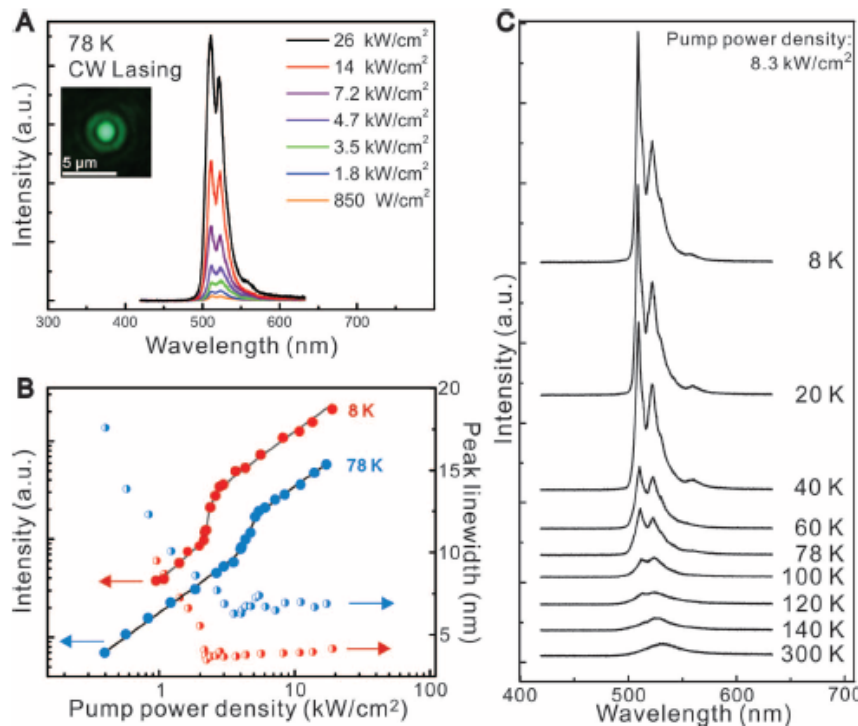
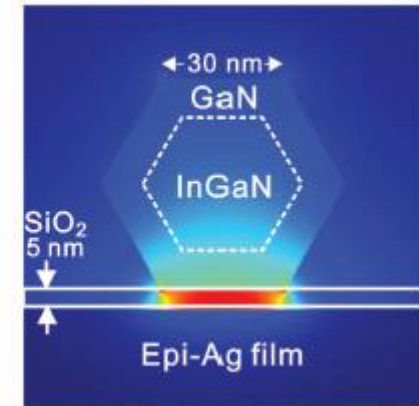
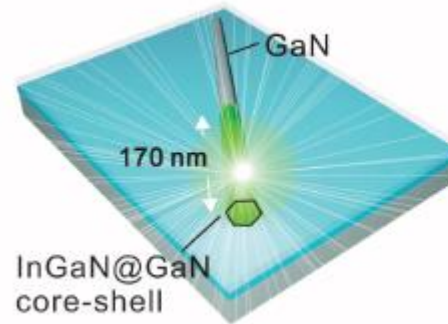
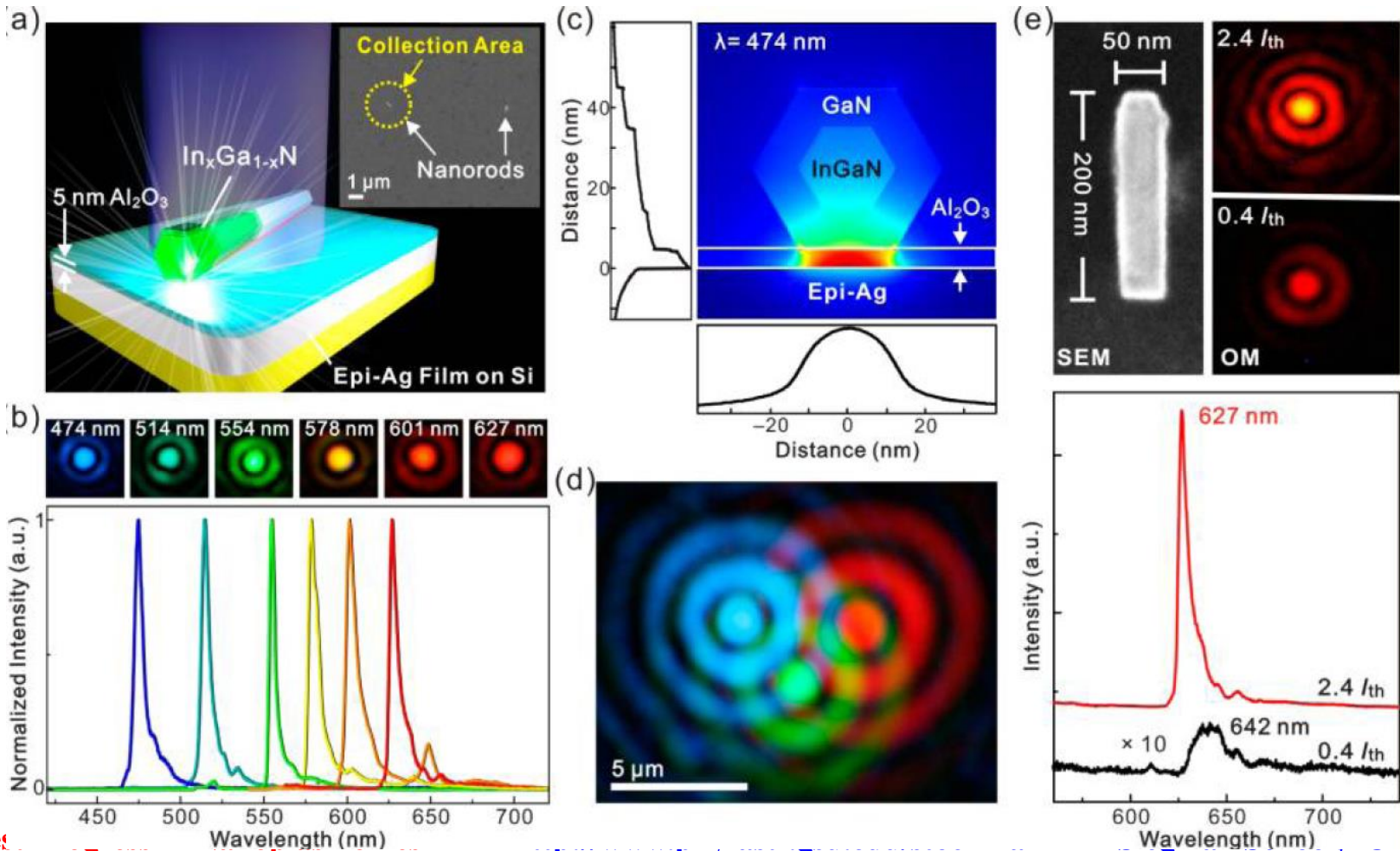


Fig. 3. (A) Lasing spectra for pumping by a CW 405-nm semiconductor diode laser. (Inset) The far-field laser spot, with contrast fringes indicative of spatial coherence resulting from lasing. a.u., arbitrary units. (B) Temperature-dependent lasing thresholds of the plasmonic cavity. The $L-L$ plots at the main lasing peak (510 nm) are shown with the corresponding linewidth-narrowing behavior when the plasmonic laser is measured at 8 K (red) and 78 K (blue), with lasing thresholds of 2.1 and 3.7 kW/cm², respectively. (C) Temperature-dependent lasing behavior from 8 to 300 K. (D) Second-order photon correlation function measurements at 8 K.

Y.-J. Lu *et al.*, Nano Lett. **14**, 4381 (2014)

All-Color Plasmonic Nanolasers with Ultralow Thresholds: Autotuning Mechanism for Single-Mode Lasing

Yu-Jung Lu,[†] Chun-Yuan Wang,[†] Jisun Kim,[‡] Hung-Ying Chen,[†] Ming-Yen Lu,^{||} Yen-Chun Chen,[⊥] Wen-Hao Chang,[⊥] Lih-Juann Chen,^{||} Mark I. Stockman,^{§,¶,||} Chih-Kang Shih,^{*,‡} and Shangjr Gwo^{*,†}



ARTICLE

Received 28 Dec 2013 | Accepted 11 Aug 2014 | Published 23 Sep 2014

DOI: 10.1038/ncomms5953

A room temperature low-threshold ultraviolet plasmonic nanolaser

Qing Zhang¹, Guangyuan Li¹, Xinfeng Liu¹, Fang Qian², Yat Li³, Tze Chien Sum^{1,4}, Charles M. Lieber⁵ & Qihua Xiong^{1,6}

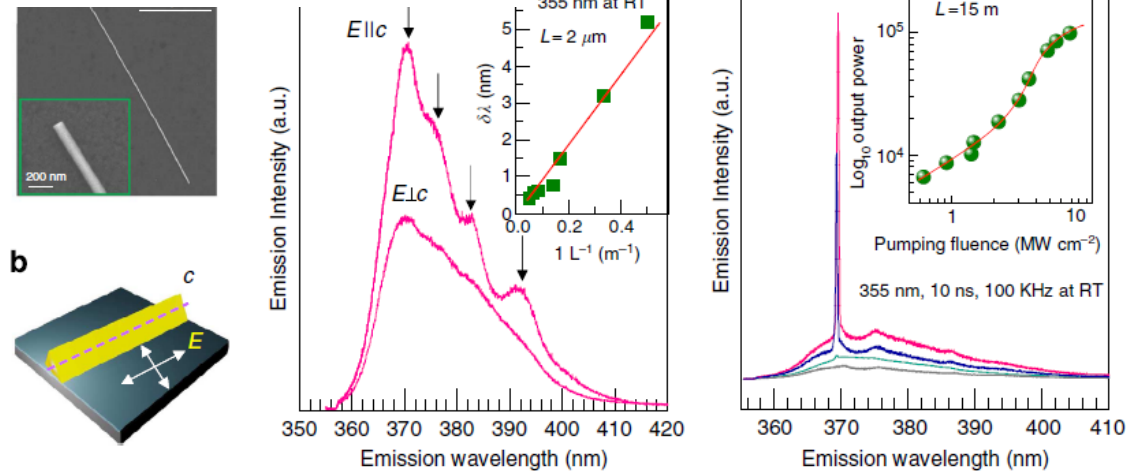
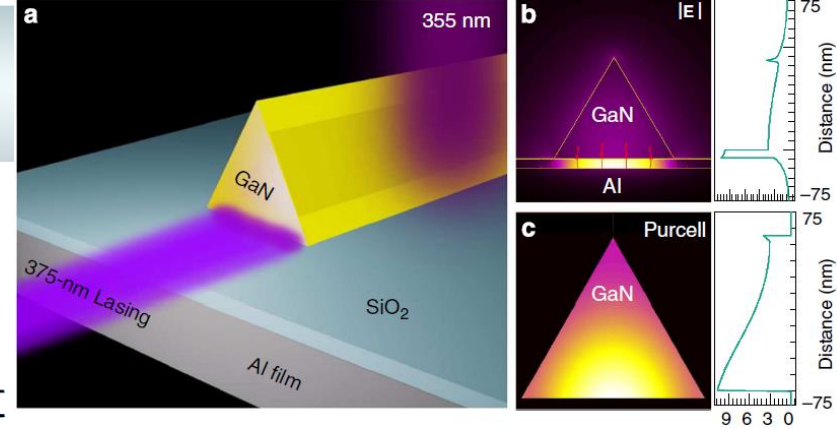


Figure 2 | Room temperature ultraviolet plasmonic lasing characterization. (a) Scanning electron microscopy (SEM) image of a GaN nanowire sitting on SiO₂/Al film. Inset: magnified scanning electron microscopy image of one end of the GaN nanowire. The nanowire length and diameter is 15 μm and 100 nm, respectively. (b) Schematic of optical measurement and polarization detection setup. c is defined as the orientation of nanowire. The incidence excitation laser is circular polarized and the focused laser beam can cover the whole nanowire. The emission scattered out from two ends is collected and the polarization property along and perpendicular to nanowire axis c is analysed. (c) Spontaneous emission of as-fabricated plasmonic device below lasing threshold at room temperature under a power fluence of 0.5 MW cm⁻². Arrows highlight the Fabry-Pérot peaks. The nanowire length is 2 μm. Inset: cavity mode spacing $\delta\lambda$ variation with nanowire length L (green dots). $\delta\lambda$ versus 1/L can be well fitted with a linear function (red curve), suggesting a high group index n_g ($n_g = \lambda^2/2L$) of 7.61 due to the high gain requirement of the plasmonic laser device. (d) Power-dependent emission spectra of the plasmonic devices. One sharp peak with a maximum full width at half maximum (FWHM) \sim 0.8 nm appears above the spontaneous emission background. The nanowire length is 15 μm. Inset: integrated emission versus pumping intensity. The S-shaped plot suggests the evolution from a spontaneous emission, amplified spontaneous emission to lasing process.

Graphene spaser

Vadym Apalkov¹ and Mark I. Stockman^{1,2,3}

¹*Department of Physics and Astronomy, Georgia State University, Atlanta, Georgia 30303, USA*

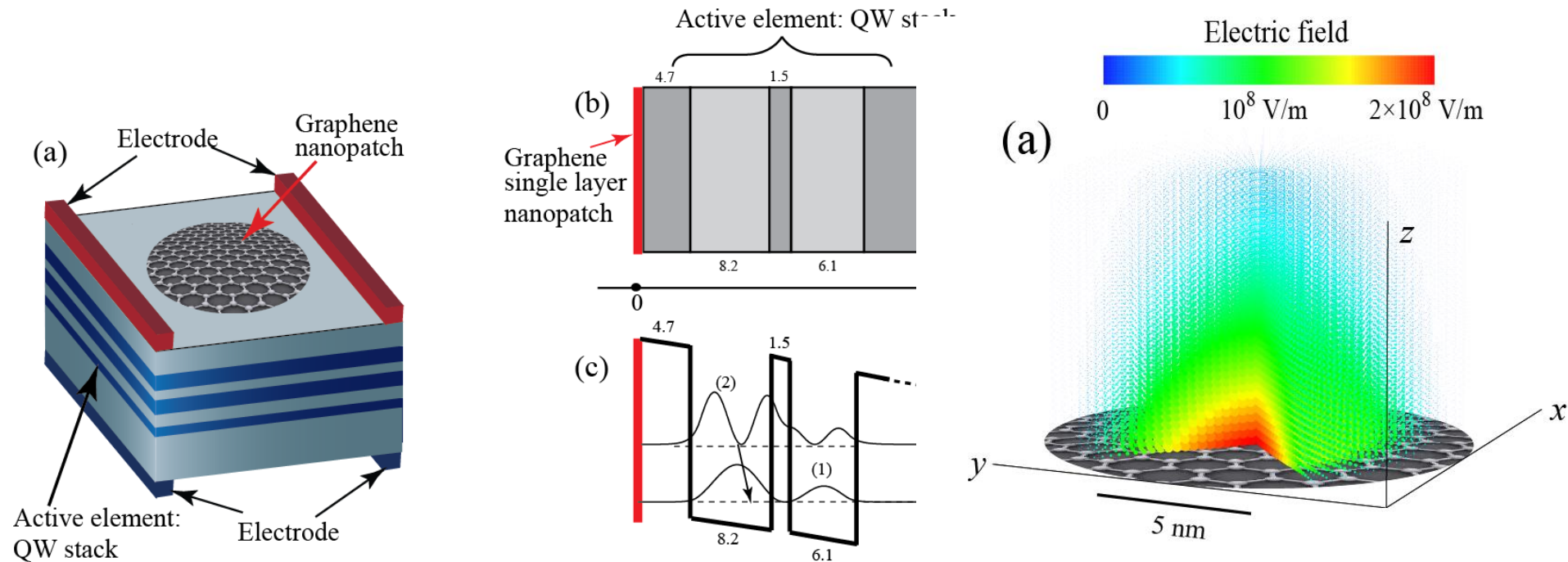
²*Fakultät für Physik, Ludwig-Maximilians-Universität,
Geschwister-Scholl-Platz 1, D-80539 München, Germany*

³*Max-Planck-Institut für Quantenoptik, Hans-Kopfermann-Strasse 1, D-85748 Garching, Germany*

(Dated: May 10, 2013)

We propose a graphene spaser, which is a coherent quantum generator of surface plasmons in nanostructured graphene. The plasmonic core of this spaser is a graphene monolayer nanopatch and its active (gain) element is a multi-quantum well system with a design similar to the design of an active element of quantum cascade laser. For realistic parameters of the multi-quantum well system, the spasing in graphene monolayer can be achieved at a finite doping of graphene and at a plasmon frequency, ≈ 0.15 eV, close to the typical frequency of intersubband transitions in multi-quantum well systems. The proposed graphene spaser will be an efficient source of intense and coherent nanolocalized fields in the mid-infrared spectral region with wide perspective applications in mid-infrared nanoscopy, nano-spectroscopy, and nano-lithography.

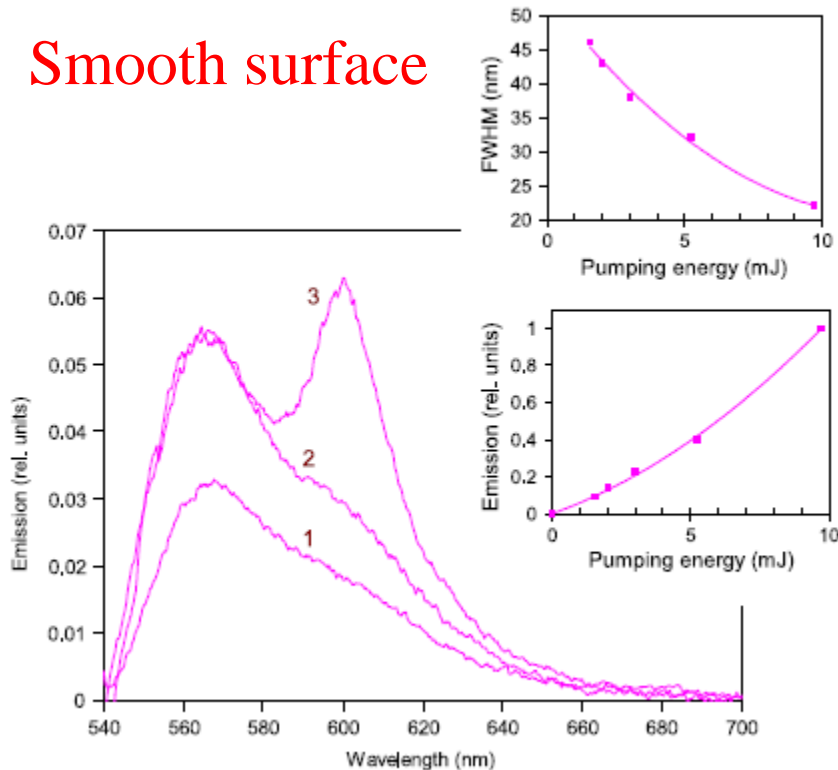
V. Apalkov and M. I. Stockman, *Proposed Graphene Nanospaser*, NPG: Light Sci. Appl. **3**, e191 (2014).



Stimulated emission of surface plasmon polaritons on smooth and corrugated silver surfaces

J K Kitor, G Zhu, Yu A Barnakov and M A Noginov

Smooth surface



Random Spaser

Rough surface

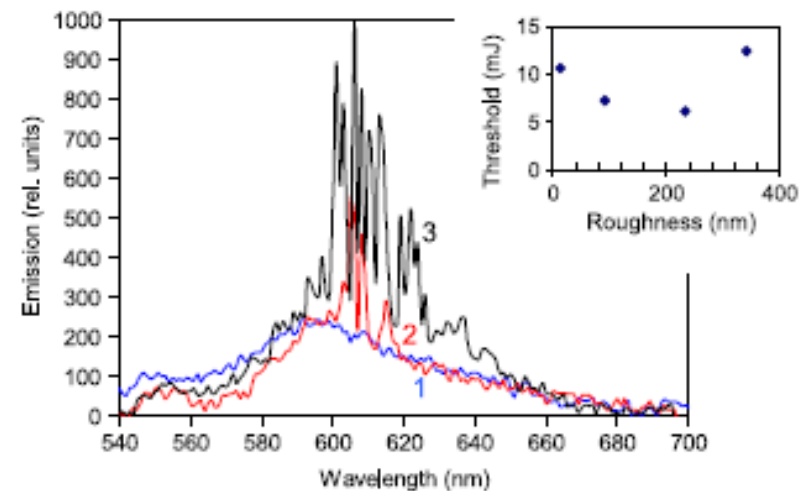
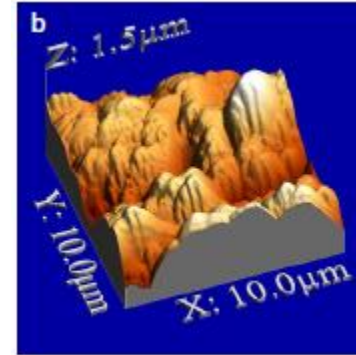


Figure 5. Emission spectra in the RB:PMMA film deposited on a roughened silver with surface roughness equal to 234 nm, pumped with 7 mJ (1), 13 mJ (2) and 20 mJ (3) laser pulses. Inset: stimulated emission threshold as a function of the surface roughness.

Surface plasmon lasing observed in metal hole arrays

Phys. Rev. Lett. **110**, 206802-1-5 (2013)

Frerik van Beijnum,¹ Peter J. van Veldhoven,² Erik Jan Geluk,² Michiel J.A. de Dood,¹ Gert W. 't Hooft,^{1,3} and Martin P. van Exter¹

¹Leiden University, Huygens Laboratory, P.O. Box 9504, 2300 RA Leiden, The Netherlands

²COBRA Research Institute, Technische Universiteit Eindhoven, Postbus 513, 5600 MB Eindhoven, The Netherlands

³Philips Research Laboratories, Prof. Holstlaan 4, 5656 AA Eindhoven, Netherlands

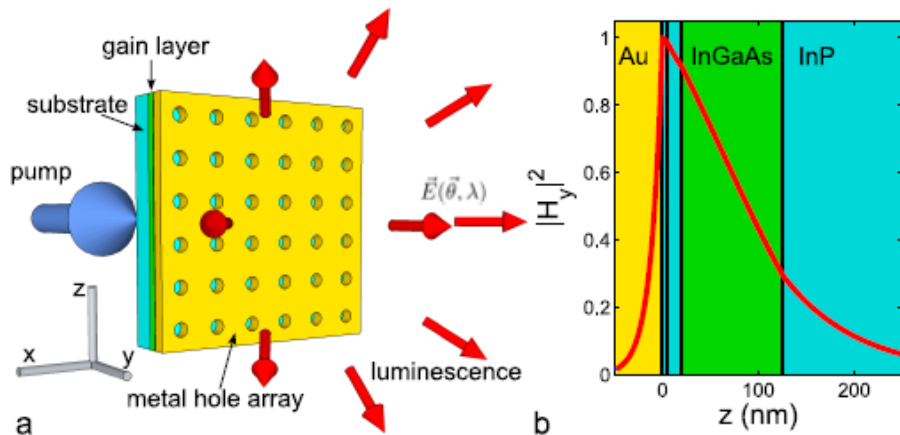
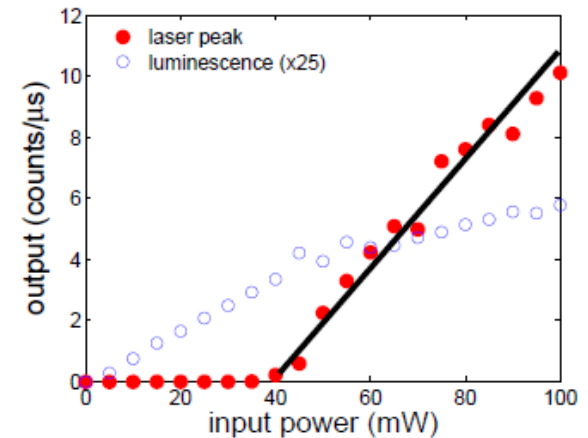
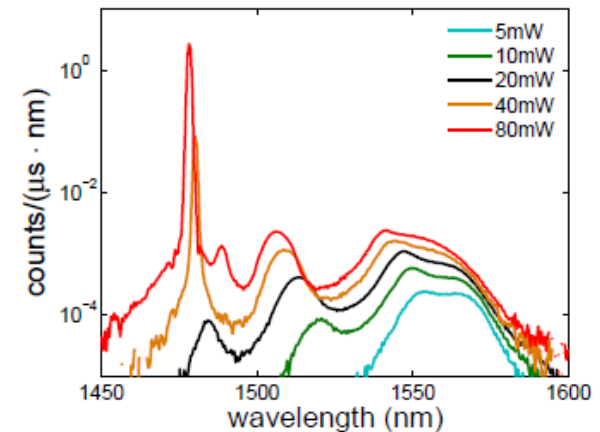
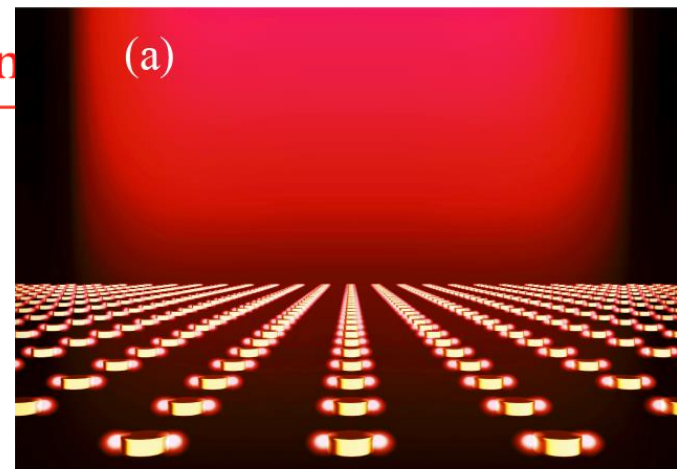


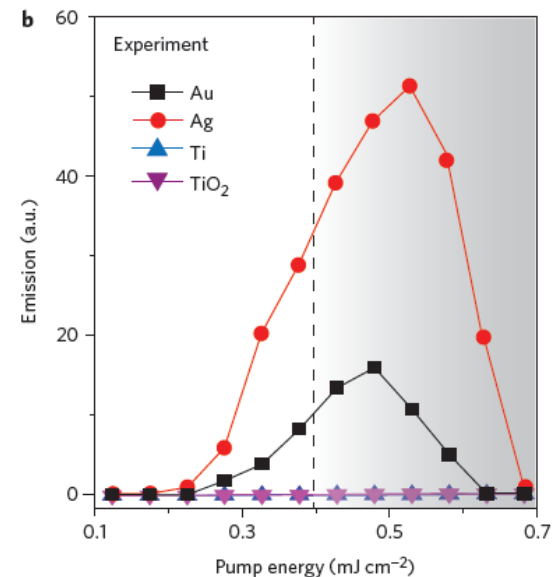
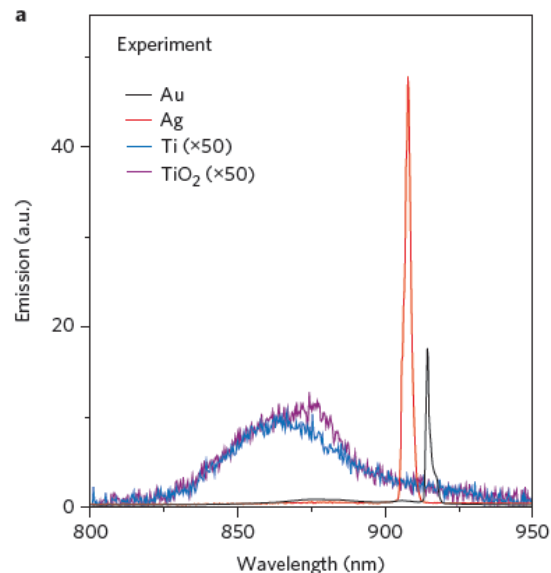
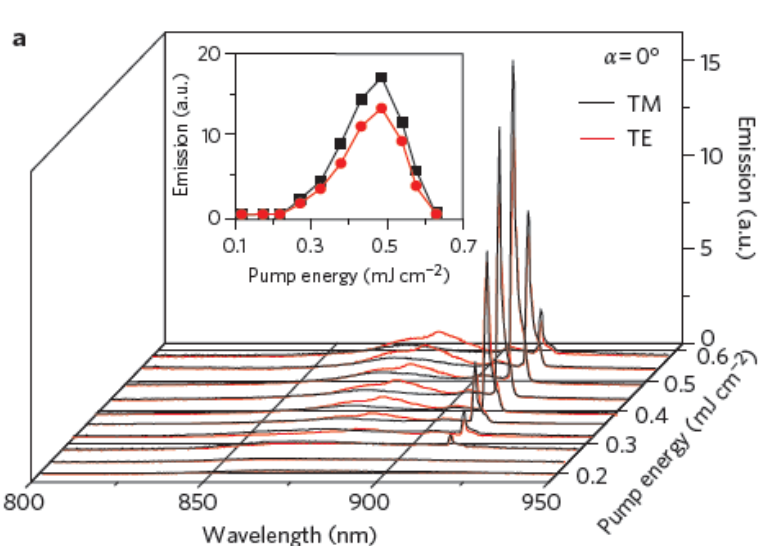
FIG. 2. (a) Luminescence spectra as a function of pump power, plotted on a semilog scale. For increasing pump power the bandwidth of the luminescence increases until the device starts lasing. Above threshold, the emission of the non-lasing resonances starts to saturate at a maximum intensity. 80 mW corresponds to $\sim 11 \text{ kW/cm}^2$ (b) The output in the lasing peak and in the luminescence in the range of 1485 – 1600 nm. The power in the lasing peak shows a clear threshold (red). The black line is a guide to the eye. The luminescence outside the lasing peak starts to level off, as expected for lasing in semiconductor devices (blue).





Lasing action in strongly coupled plasmonic nanocavity arrays

Wei Zhou^{1†}, Montacer Dridi², Jae Yong Suh², Chul Hoon Kim^{2,3†}, Dick T. Co^{2,3},
Michael R. Wasielewski^{2,3}, George C. Schatz² and Teri W. Odom^{1,2,3*}



Ultrafast plasmonic nanowire lasers near the surface plasmon frequency

Themistoklis P. H. Sidiropoulos^{1*}, Robert Röder², Sebastian Geburt², Ortwin Hess¹, Stefan A. Maier¹, Carsten Ronning² and Rupert F. Oulton^{1*}

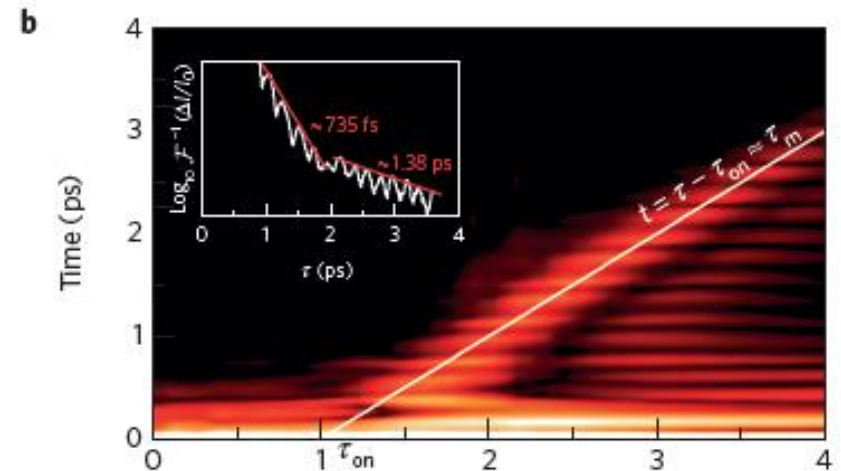
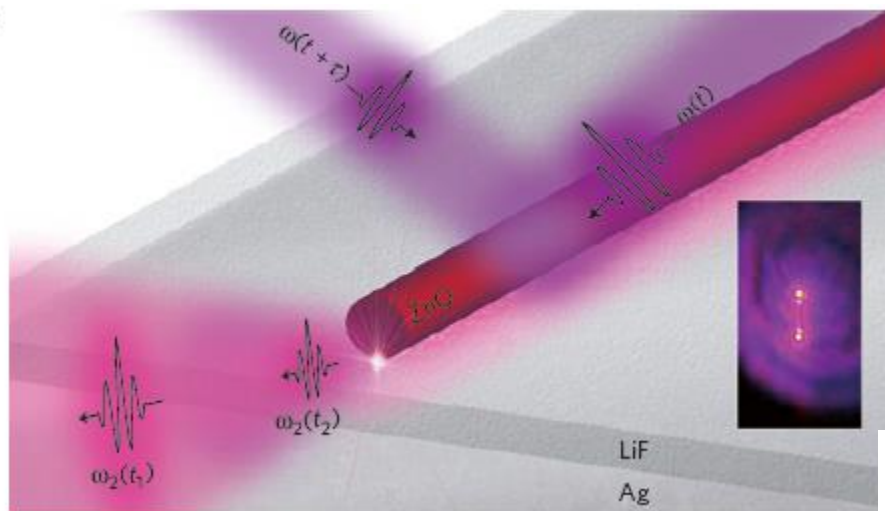
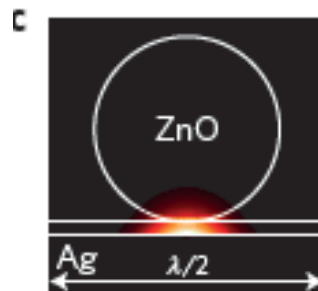


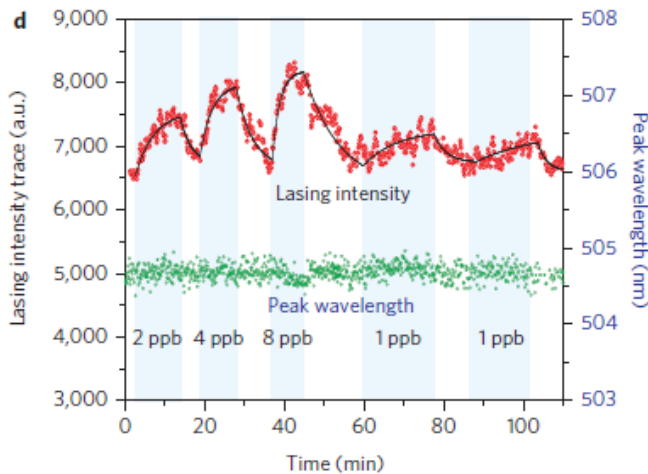
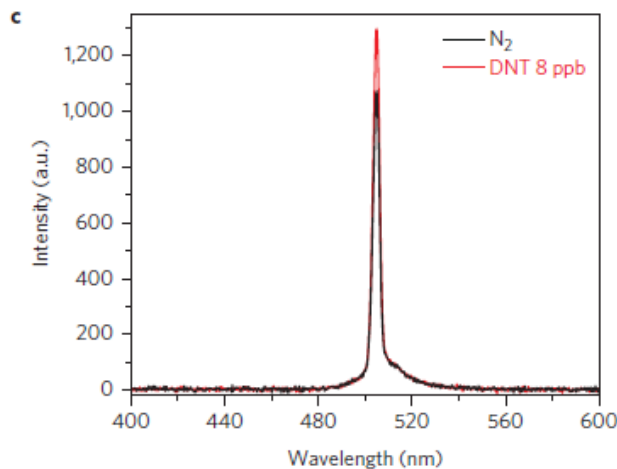
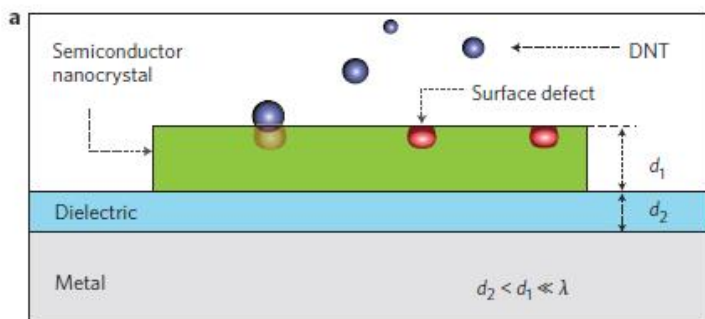
Figure 5 | Measured spectra versus double-pump pulse delay for the plasmonic nanowire laser and its Fourier transform. a, Normalized difference spectrum, $\Delta I(\lambda, \tau)/I_0(\lambda) - I(\lambda, \tau)/I_0(\lambda) - 1$, of the plasmonic nanowire laser for $\tau \geq 0$, where $I(\lambda, \tau)$ is the spectrum under double-pump excitation and $I_0(\lambda)$ is the single strong pump pulse spectrum. The two upper panels show the $\Delta I/I_0$ spectra for the pulse delays, $\tau = 2.0$ ps and $\tau = 3.1$ ps, indicating the increasing spectral modulation frequency with pulse delay. **b**, Fourier transform of each spectrum shown in **a** versus pulse delay. The white trend line follows $t = \tau - \tau_{\text{on}} \approx \tau_m$, indicating a turn-on time of $\tau_{\text{on}} = 1.1$ ps. The inset shows the amplitude decay of the Fourier transform along the white trend line, with linear fits (red lines) to the modulation peaks. The presented data in this figure correspond to measurements at the highest pump power (situation i) shown in Fig. 4a.



Explosives detection in a lasing plasmon nanocavity

Ren-Min Ma^{1†}, Sadao Ota^{1†}, Yimin Li¹, Sui Yang¹ and Xiang Zhang^{1,2*}

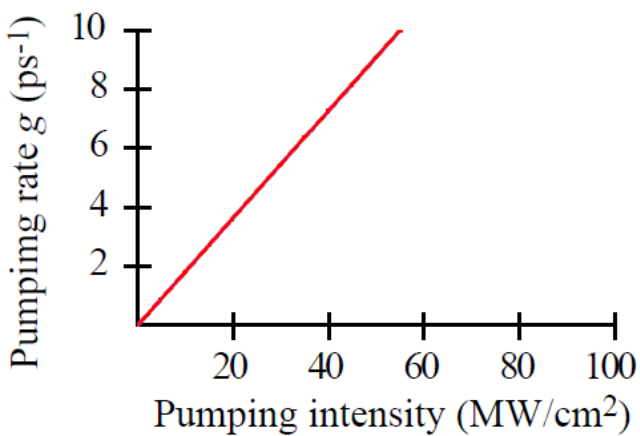
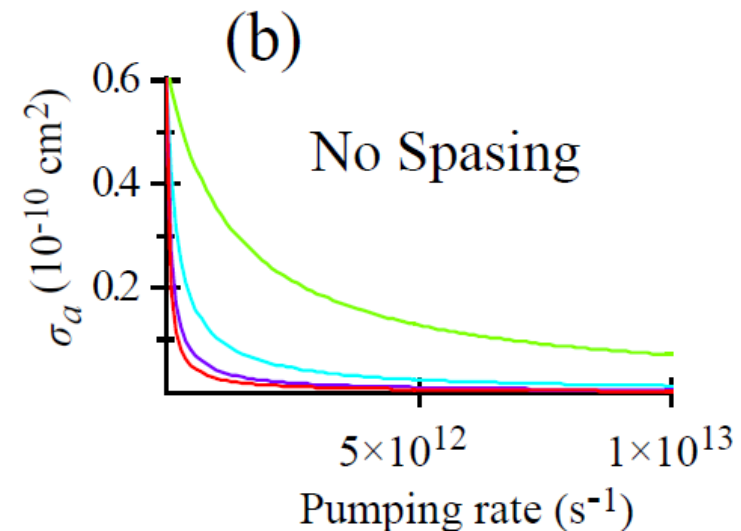
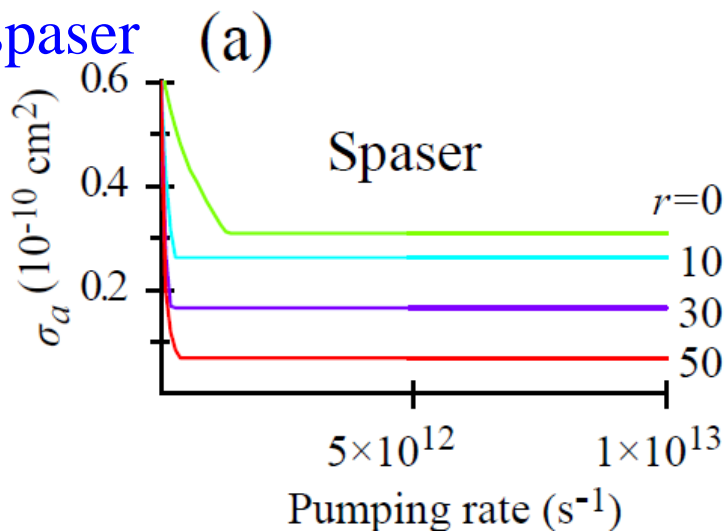
¹NSF Nanoscale Science and Engineering Centre, 3112 Etcheverry Hall, University of California, Berkeley, California 94720, USA, ²Materials Sciences Division, Lawrence Berkeley National Laboratory, 1 Cyclotron Road, Berkeley, California 94720, USA,



Explosive (DNT) detection

Applications in Biomedicine: Why spaser is efficient as fluorescent, photothermal and photoacoustic agent? It does not saturate!

Absorption cross section as a function of the pumping rate for different loads r of spaser



H. Koochaki and M. Stockman (In preparation)

Spaser as Versatile Biomedical Tool

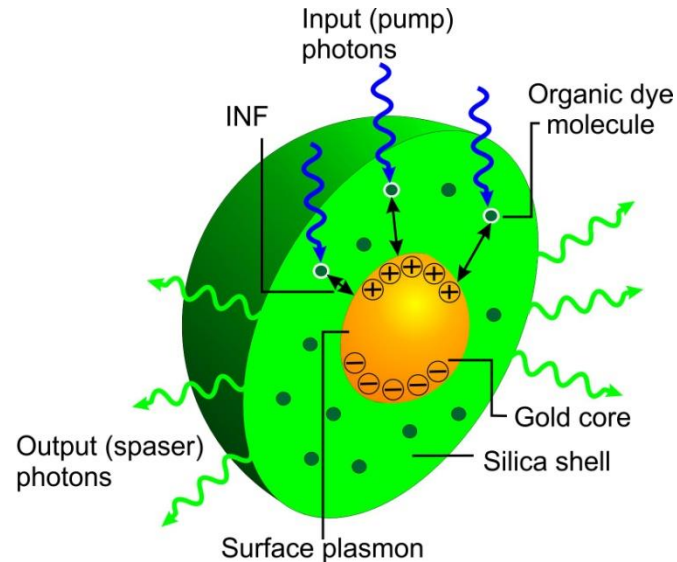
Ekaterina I. Galanzha,¹ Robert Weingold,¹ Dmitry A. Nedosekin,¹ Mustafa Sarimollaoglu,¹
Alexander S. Kuchyanov,² Roman G. Parkhomenko,³ Alexander I. Plekhanov,² Mark I.
Stockman⁴, Vladimir P. Zharov¹

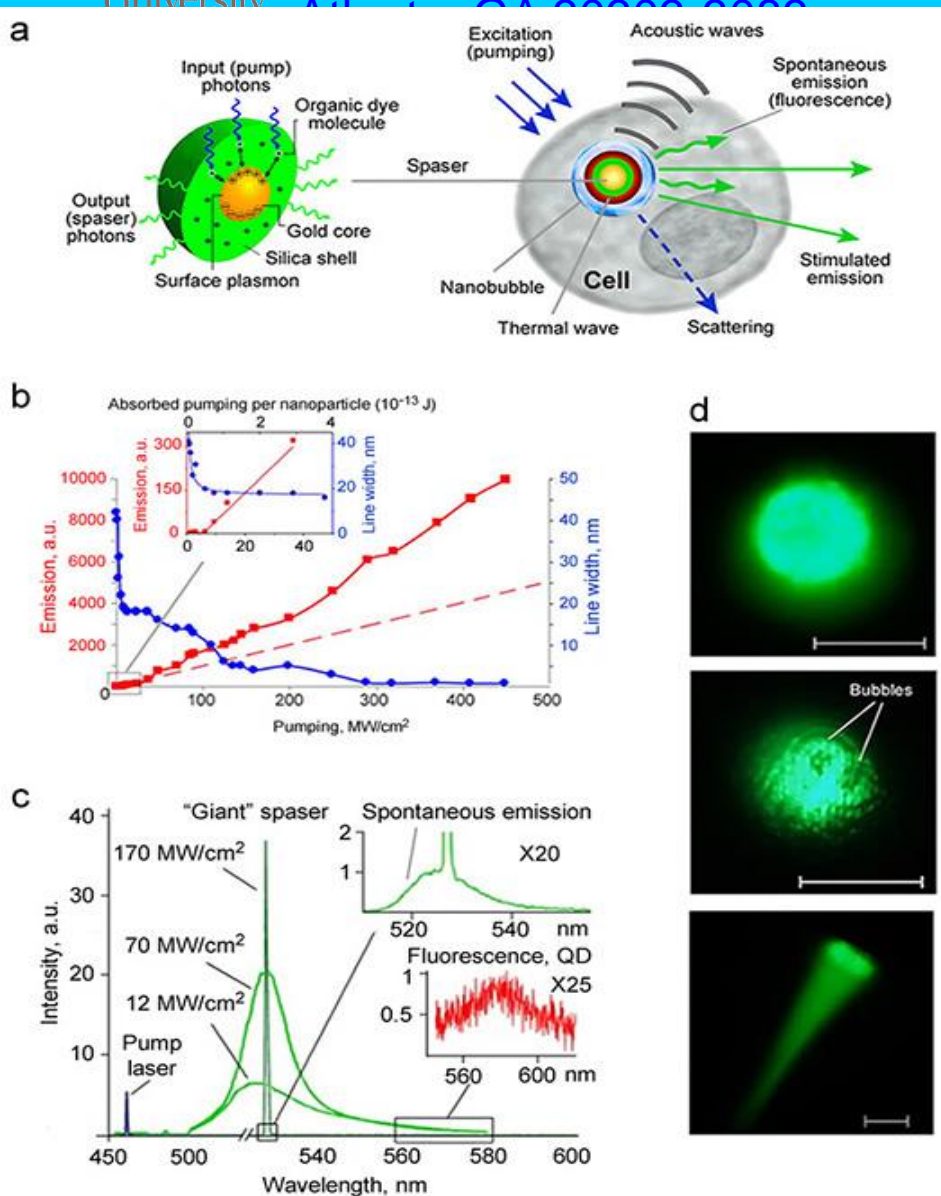
¹Winthrop P. Rockefeller Cancer Institute, Arkansas Nanomedicine Center, University of
Arkansas for Medical Sciences, Little Rock, Arkansas 72205

²Institute of Automation and Electrometry of the Siberian Branch of the Russian Academy of
Science, Koptug Ave. 1, 630090 Novosibirsk, Russia

³Nikolaev Institute of Inorganic Chemistry of the Siberian Branch of the Russian Academy of
Science, Lavrentiev Ave. 3, 630090 Novosibirsk, Russia

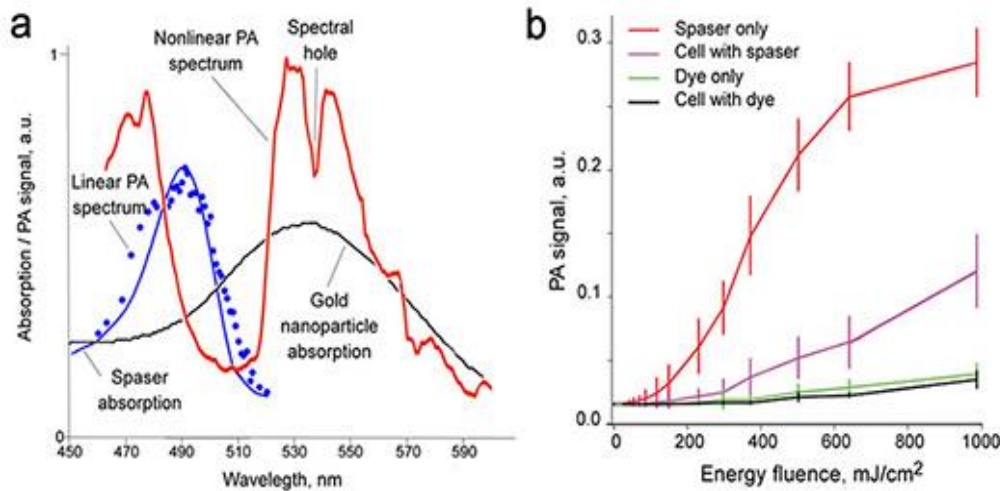
⁴Center for Nano-Optics and Department of Physics and Astronomy, Georgia State University,
29 Peachtree Center Ave., Atlanta, GA 30302, USA





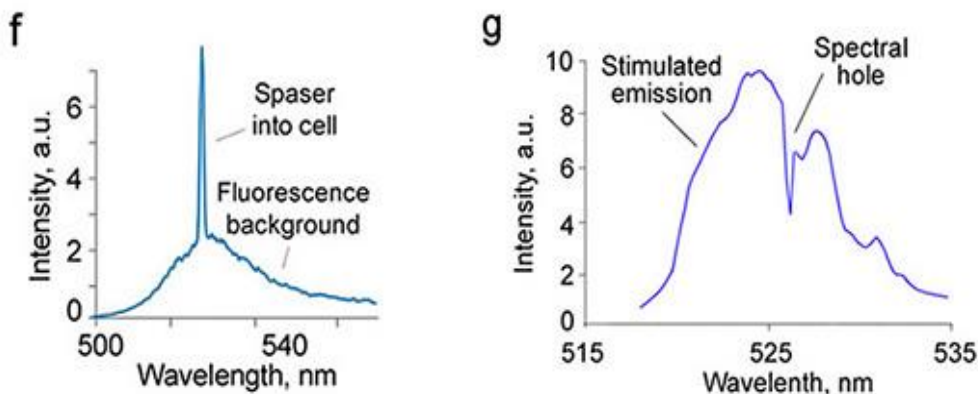
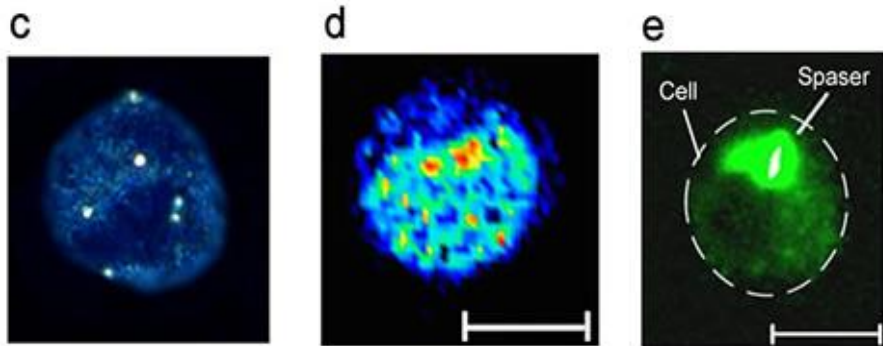
Spaser for biological applications

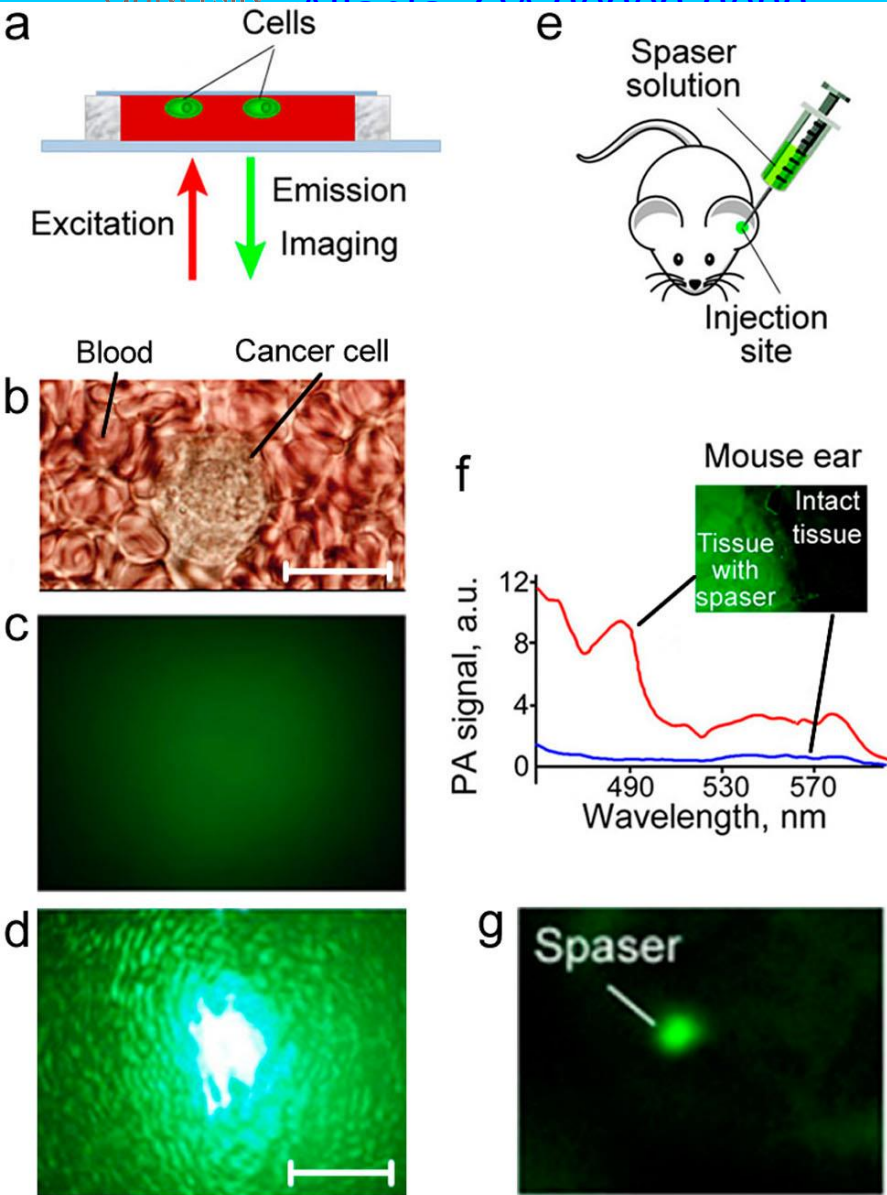
a, Schematic of spaser as multifunctional intracellular nanoprobe. **b**, Stimulated emission in spaser suspension. **c**, Radiation spectrum of spaser in suspension at 528 nm at different pump intensities. **d**, Spatially homogenous spaser's emission at a relatively low pump intensity (30 MW/cm², 120- μ m thick spaser's suspension); **Middle**: emission during the bubble formation around overheated spasers (150 MW/cm²); **Bottom**: "directional" spaser emission in the presence of two large bubbles (200 MW/cm²). Scale bars, 10 μ m.



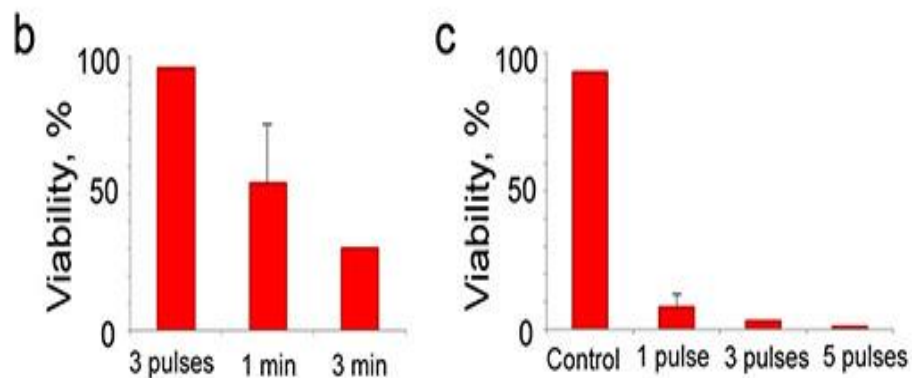
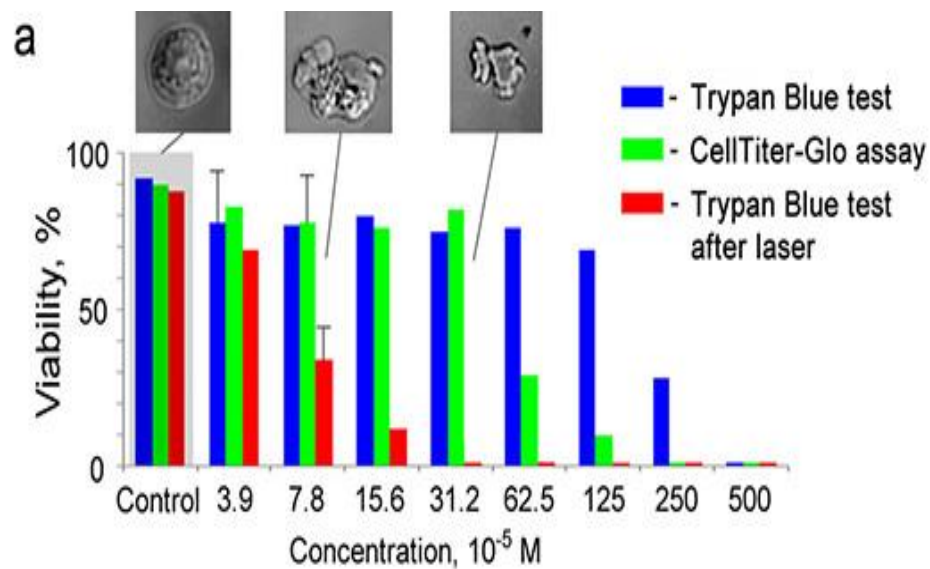
Nanoplasm

Photoacoustic (PA) and photothermal (PT) spectral microscopy of spasers. **a**, Absorption spectra, and linear and nonlinear PA spectra of spaser in suspension at laser energy fluence of 20 mJ/cm² and 150 mJ/cm², respectively. **b**, PA signal dependence on laser pump energy fluence for dye and spaser in suspension and into cells. **c-e**, Images of single cancer cell with spasers loaded through endocytosis. **(c)**-scattering (dark field), **(d)**-photothermal (PT); **(e)**-stimulated emission for local irradiated cell zone in background of conventional fluorescence image. **f**, Spectral peak from single cancer cell with spasers at relatively low energy fluence (80 mJ/cm²). Scale bars, 10 μm. **g**, Spectral peak single cancer cell with spasers showing spectral hole burning in stimulated emission spectra at moderate energy fluence (135 mJ/cm²).





Imaging of spasers in viable cells *in vitro* and in biotissue *in vivo*. **a**, Schematic *in vitro*. **b**, Optical transmission image. **c, d**, Fluorescence imaging using conventional optical source (lamp) of blood with cancer cells at depth of ~ 1 mm (**top**) and spaser emission from single cancer cell at depth of 1 mm (**bottom**). **e**, Schematic of intradermal injection of spaser suspension into top layer of mouse ear tissue. **f**, PA identification of spasers in ear tissue using laser spectral scanning (**top**). Laser parameters: beam diameter $15 \mu\text{m}$, fluence $20 \text{ mJ}/\text{cm}^2$. **g**, Spaser emission through $\sim 250 \mu\text{m}$ ear tissue. Pump parameters: beam diameter: $10 \mu\text{m}$; intensity, $30 \text{ MW}/\text{cm}^2$.



Demonstration of spaser as theranostic agent. a, Cell viability tests for different spaser concentration using two various kits without (blue, green) and after (red) laser irradiation (100 mJ/cm^2 , 1 Hz, 3min). Inset: intact cell (**left**) and cells labeled with spasers at different concentration (middle and right) after laser irradiation. **b,** Viability test for concentration 15.6×10^{-5} M as a function of laser exposure time (3s [3 pulses], 1 min, and 3 min); **c,** Viability test for concentration 15.6×10^{-5} M as a function of laser pulse number (1, 3 and 5) showing that even single laser pulse at fluence of 500 mJ/cm^2 is sufficient for significant damage of cancer cells labeled by spasers. The average SD for each column is 15-20%.

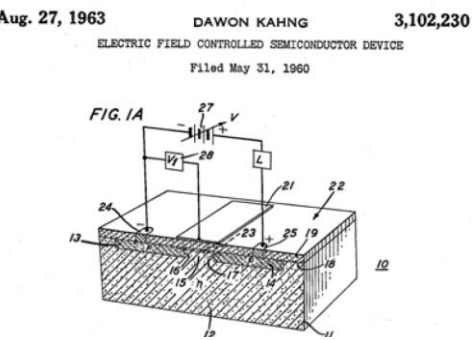
The most important technological application: Information processing

P. Packan et al., in 2009 IEEE International Electron Devices Meeting (IEDM), *High Performance 32nm Logic Technology Featuring Second Generation High-K + Metal Gate Transistors* (Baltimore, MD, 2009), Vol. IEDM09-662, p. 28.4.1-28.4.4

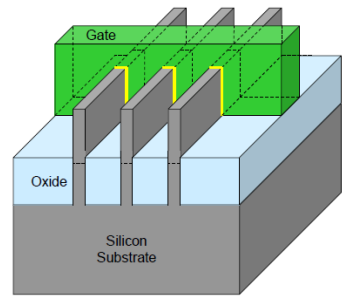
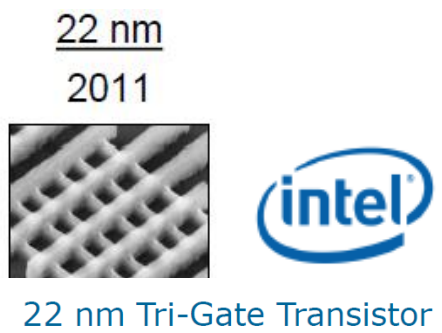
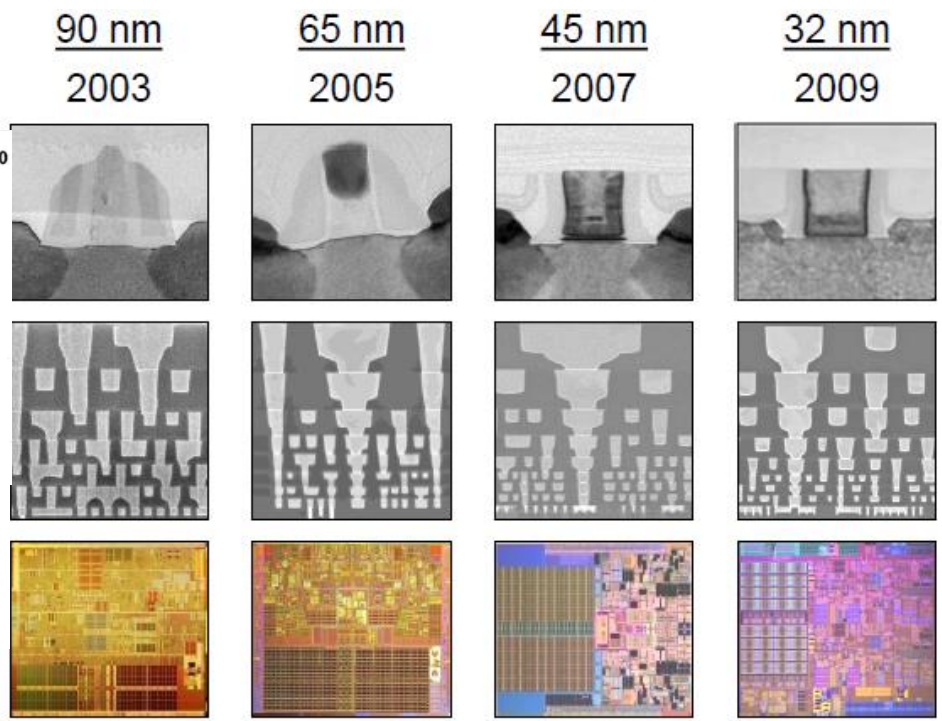
Abstract:

A 32nm logic technology for high performance microprocessors is described. 2nd generation high-k + metal gate transistors provide record drive currents at the tightest gate pitch reported for any 32 nm or 28nm logic technology. NMOS drive currents are 1.62mA/um Idsat and 0.231mA/um Idlin at 1.0V and 100nA/um Ioff. PMOS drive currents are 1.37mA/um Idsat and 0.240mA/um Idlin at 1.0V and 100nA/um Ioff. The impact of SRAM cell and array size on Vccmin is reported.

MOSFET US Patent



Speed ~ 100-300 GHz
Low resistance to ionizing radiation



Tri-Gate transistors can have multiple fins connected together to increase total drive strength for higher performance

Processor speed :

$$f_{max} = I_{drive} / (C_{Intercon} \Delta U) \sim 3 \text{ GHz}$$

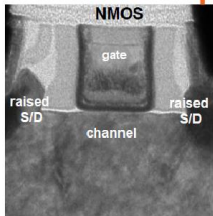
Transistor speed is not a limiting factor!

Charging the interconnects is.

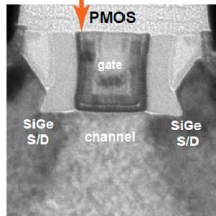
Concept of ~300 GHz processor unit with ~1% energy cost per flop

Today C-MOS Technology

Electric interconnect (Copper wire)



$$\tau = RC \sim \epsilon\sigma \frac{L^2}{r^2}$$

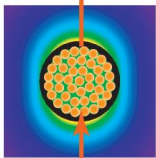


Charging time does not depend on scale

Near-future C-MOS Technology with on-chip plasmonic interconnects

Nanoplasmonic on-chip interconnect (Copper wire)

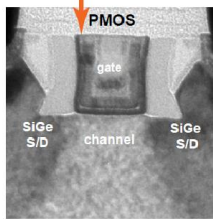
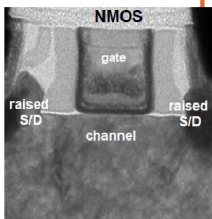
Spaser pumped by transistor



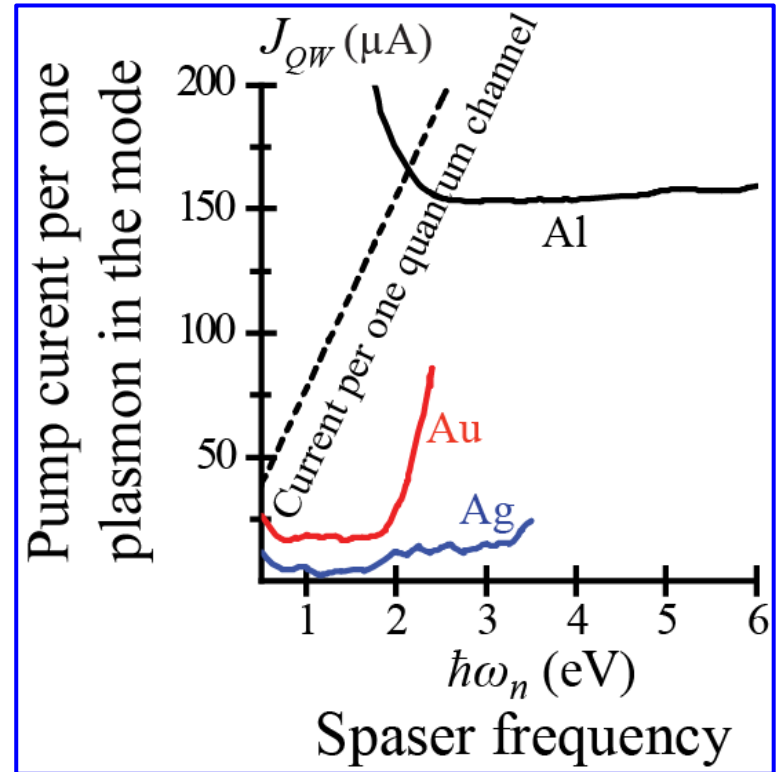
Phototransistor 

No electric charging of interconnects!

C-MOS Transistors are not connected electrically



Nanospaser with electric excitation ("pumping") does not exist as of today yet, but fundamentally it is entirely possible



D. Li and M. I. Stockman, *Electric Spaser in the Extreme Quantum Limit*, Phys. Rev. Lett. **110**, 106803-1-5 (2013)

CONCLUSIONS

- **Spasers are plasmonic nanolasers that have been demonstrated to generate in a wide range of optical frequencies: from near-UV to near-IR**
- **Various designs of spasers have been implemented:**
 - **metal core/gain shell**
 - **gain semiconductor nanorod over continuous metal nanofilm**
 - **Rough metal nanofilm/gain dye nanolayer**
 - **metal/gain semiconductor/metal**
 - **lasing spaser of periodic array of nanoholes in a metal nanofilm with a semiconductor gain nanofilm over it**
 - **lasing spaser of a periodic array of metal nanoparticles on a gain dye nanolayer**
- **Mid IR nanospaser on graphene has been proposed**
- **First applications of spasers in explosives detection and cancer diagnostics and treatment have been introduced**

A dramatic sunset over a body of water. The sky is filled with dark, heavy clouds, with a bright orange and red glow from the setting sun breaking through. In the foreground, the dark silhouettes of buildings are visible, with a few small lights glowing from windows. The water is dark, and numerous sailboats are scattered across the horizon, their sails catching the low light. The overall mood is somber and reflective.

The End